

44691

National Library
of CanadaBibliothèque nationale
du Canada

Canadian Theses Division / Division des thèses canadiennes

Ottawa, Canada
K1A 0N4**PERMISSION TO MICROFILM — AUTORISATION DE MICROFILMER**

- Please print or type — Écrire en lettres moulées ou dactylographier

Full Name of Author — Nom complet de l'auteur

Craig Stewart Banks

Date of Birth — Date de naissance

December 17, 1952

Country of Birth — Lieu de naissance

Canada

Permanent Address — Résidence fixe

8703-147 Street
Edmonton, Alberta

Title of Thesis — Titre de la thèse

Geochronology, General Geology and Structure
of Hill Island Lake - Tazin Lake Areas

University — Université

Alberta (Edmonton)

Degree for which thesis was presented — Grade pour lequel cette thèse fut présentée

Master of Science

Year this degree conferred — Année d'obtention de ce grade

1980

Name of Supervisor — Nom du directeur de thèse

H. Baadsgaard

Permission is hereby granted to the NATIONAL LIBRARY OF CANADA to microfilm this thesis and to lend or sell copies of the film.

The author reserves other publication rights, and neither the thesis nor extensive extracts from it may be printed or otherwise reproduced without the author's written permission.

L'autorisation est, par la présente, accordée à la BIBLIOTHÈQUE NATIONALE DU CANADA de microfilmer cette thèse et de prêter ou de vendre des exemplaires du film.

L'auteur se réserve les autres droits de publication; ni la thèse ni de longs extraits de celle-ci ne doivent être imprimés ou autrement reproduits sans l'autorisation écrite de l'auteur.

Date

March 24, 1980

Signature

Craig S. Banks



National Library of Canada
Collections Development Branch

Canadian Theses on
Microfiche Service

Bibliothèque nationale du Canada
Direction du développement des collections

Service des thèses canadiennes
sur microfiche

NOTICE

The quality of this microfiche is heavily dependent upon the quality of the original thesis submitted for microfilming. Every effort has been made to ensure the highest quality of reproduction possible.

If pages are missing, contact the university which granted the degree.

Some pages may have indistinct print especially if the original pages were typed with a poor typewriter ribbon or if the university sent us a poor photocopy.

Previously copyrighted materials (journal articles, published tests, etc.) are not filmed.

Reproduction in full or in part of this film is governed by the Canadian Copyright Act, R.S.C. 1970, c. C-30. Please read the authorization forms which accompany this thesis.

**THIS DISSERTATION
HAS BEEN MICROFILMED
EXACTLY AS RECEIVED**

AVIS

La qualité de cette microfiche dépend grandement de la qualité de la thèse soumise au microfilmage. Nous avons tout fait pour assurer une qualité supérieure de reproduction.

S'il manque des pages, veuillez communiquer avec l'université qui a conféré le grade.

La qualité d'impression de certaines pages peut laisser à désirer, surtout si les pages originales ont été dactylographiées à l'aide d'un ruban usé ou si l'université nous a fait parvenir une photocopie de mauvaise qualité.

Les documents qui font déjà l'objet d'un droit d'auteur (articles de revue, examens publiés, etc.) ne sont pas microfilmés.

La reproduction, même partielle, de ce microfilm est soumise à la Loi canadienne sur le droit d'auteur, SRC 1970, c. C-30. Veuillez prendre connaissance des formules d'autorisation qui accompagnent cette thèse.

**LA THÈSE A ÉTÉ
MICROFILMÉE TELLE QUE
NOUS L'AVONS REÇUE**

THE UNIVERSITY OF ALBERTA

Geochronology, General Geology and Structure of Hill Island
Lake- Tazin Lake Areas

by



Craig S. Banks

A THESIS

SUBMITTED TO THE FACULTY OF GRADUATE STUDIES AND RESEARCH
IN PARTIAL FULFILMENT OF THE REQUIREMENTS FOR THE DEGREE

OF Master of Science

IN

Geology

Department of Geology

EDMONTON, ALBERTA

Spring 1980

THE UNIVERSITY OF ALBERTA
FACULTY OF GRADUATE STUDIES AND RESEARCH

The undersigned certify that they have read, and recommend to the Faculty of Graduate Studies and Research, for acceptance, a thesis entitled Geochronology, General Geology and Structure of Hill Island Lake- Tazin Lake Areas submitted by Craig S. Banks in partial fulfilment of the requirements for the degree of Master of Science in Geology.

..... *H. Boadsgaard*

Supervisor

..... *R. St. Lambert*

..... *R. A. Brown*

..... *G. L. Cummins*

Date..... *February 14, 1980*

Abstract

The results of a geochronologic study of the Hill Island Lake and Tazin Lake area using K-Ar dating of biotite, muscovite and hornblende gives K-Ar apparent ages of 1800 ma to 2620 ma within a larger area metamorphosed at 1800 ma to 1900 ma. The wide spread of apparent ages suggests deep burial, uplift and slow cooling with the possibility of a number of events resetting the K-Ar ages. These events which are mainly deformational and thermal, may have occurred at 2530 ma, 2450 ma, 2360 ma, 2200 ma, 1950 ma and 1800 ma. The extent of basement not reset by post-1900 ma events, otherwise known as the inlier, is near the 2200 ma biotite isothermal line (line of equal K-Ar age), and covers an area of about 2800 square kilometers. The resetting of 2200 ma apparent ages to 1800 ma biotite apparent ages takes place within about 20 kilometers of the 2200 ma isotemp. There has been some pre-2200 ma deformational and thermal activity in the area. These events include a strong thermal pulse and intrusion of granites, aplite granites and pegmatites at 2533 ± 15 ma. Following this, there may have been a regional thermal pulse at about 2450 ma from the distribution of hornblende apparent ages. This was accompanied by strong uplift particularly in the south end of the inlier. Late pegmatite intrusion at 2338 ± 25 ma is associated with partial to complete resetting of hornblende and biotite K-Ar apparent ages. In addition, a post-2250 ma, pre-2200 ma event may have reset biotite ages regionally,

appearing as an age distribution peak on the K-Ar age histograms. The apparent ages were not reset at the south end of the inlier at this time indicating a high crustal level for this part of the inlier.

During post-2000 ma times the basement complex had been uplifted to a high level and was shedding sediments to the south and possibly to the west as determined from the age and source directions for granitic gneiss cobbles found to the south and west. Due to their higher crustal level, competence, dry nature and distance from any major thermal activity, these rocks escaped post-2000 ma thermal metamorphism showing only some late deformation in the form of mylonitization and crushing along fault zones.

Acknowledgements

I would like to thank Drs. Baadsgaard and Lambert for valuable assistance and discussion on both technical and theoretical points. I would also like to thank Steve Launspach for invaluable assistance on the microprobe, Edata program and calculations of amphibole composition. I would like to thank Guy Bonnet for assistance with technical aspects and Chris Van Dyke for the time spent in drafting and the use of his computer drafting program.

Table of Contents

Chapter	Page
I. Introduction.....	1
A. Location, Objectives and Previous Work.....	1
Location and Access.....	1
Physiography.....	2
Objectives.....	2
Previous Work.....	3
Geochronology of Surrounding Areas.....	6
B. Geology, Structure and Metamorphism.....	10
General Geology.....	10
Structure, Magnetics and Metamorphism.....	15
C. The Retention of Radiogenic Argon by minerals...19	
II. Results and Interpretations.....	23
A. Results.....	23
B. Interpretations.....	28
C. Conclusions and Discussion.....	51
Speculations.....	57
Bibliography.....	60
Appendix.....	68
Sample Preparation.....	68
Potassium determinations.....	68
Argon determinations.....	68
Spikes, Reagents and Constants.....	69
Microprobe Analysis.....	69

Error Analysis.....84
Thin Section Descriptions.....84

List of Tables

Table.....Page

- 1 Potassium Argon data for biotite, muscovite, and24
whole rock, from the Hill Island Lake Area, N.W.T.
- 2 Potassium Argon data for hornblende from the.....26
Hill Island Lake Area, N.W.T.
- 3 Composition Correction For Amphiboles.....27
- 4 A tectonometamorphic sequence of events for.....54
the inlier in the Hill Island Lake-Tazin Lake Areas.
- 5 Composition of Amphiboles.....70

List of Figures

Figure.....	Page
1 Location.....	1
2 Hill Island Lake K-Ar Ages ma.....	28
3 Hill Island Lake K-Ar Ages ma.....	29
4 Hill Island Lake and Tazin Lake K-Ar Ages ma.....	29
5 Biotite Apparent Ages vs. Hornblende Apparent Ages.....	32
6 Geology, Geochronology, and Structure of Hill Island Lake and Tazin Lake Areas.....	33
7 Age distribution of structural data.....	39
8 Distribution of Hill Island Lake amphiboles in the..... composition range: tremolite-ferrotremolite- tschermakite-ferrotschermakite	43
9 Distribution of Hill Island Lake amphiboles in the..... composition range: pargasite-ferropargasite-	44

magnesiohastingsite-hastingsite.

- 10 Distribution of Hill Island Lake amphiboles in the.....45
composition range: edenite-ferroedenite-
(pargasite+magnesiohastingsite)-
(ferropargasite+hastingsite).
- 11 Distribution of Hill Island Lake amphiboles in the.....46
composition range: tremolite-ferrotremolite-
(pargasite+magnesiohastingsite)-
(ferropargasite+hastingsite).
- 12 Distribution of Hill Island Lake amphiboles in the.....47
composition range: tschermakite-ferrotschermakite-
(pargasite+magnesiohastingsite)-
(ferropargasite+hastingsite).
- 13 $2+Fe/(2+Fe+Mg)$ vs. Amphibole Apparent Ages.....49
- 14 $\%(Mg+(VI)Al/(Mg+(VI)Al+Fe))$ vs. Amphibole Apparent.....50
Ages.
- 15 Approximate Sequence of Events.....53

List of Plates

Plate.....	Page
I. Hornblende with contaminant.....	96
II. Hornblende, magnetite, biotite and quartz..... intergrowth.	98
III. Hornblende, biotite intergrowth and biotite in..... plagioclase.	100
IV. Hornblende with intergrowth of minerals.....	102
V. Polymetamorphism and biotite alteration.....	104
VI. Amphibolite facies retrogression and late..... alteration.	106
VII. Granulite facies retrogression and deformation.....	108

List of Maps

Map.....Page

1 Geology, Geochronology and Structure of Hill ...pocket
Island Lake and Tazin Lake

2 Geochronologic Interpretation and Geology of ...pocket
Hill Island Lake and Structure of Tazin Lake

I. Introduction

A. Location, Objectives and Previous Work

Location and Access

The Hill Island Lake area is situated in the southeast District of Mackenzie immediately north of the boundary between Saskatchewan and the North West Territories, just north of the northwest corner of Saskatchewan. It constitutes the National Topographic System area 75-C and lies about 60 miles north-northwest of Uranium City, Saskatchewan, and 120 miles east-northeast of Fort Smith, North West Territories, (see figure 1 and map 1 in pocket).

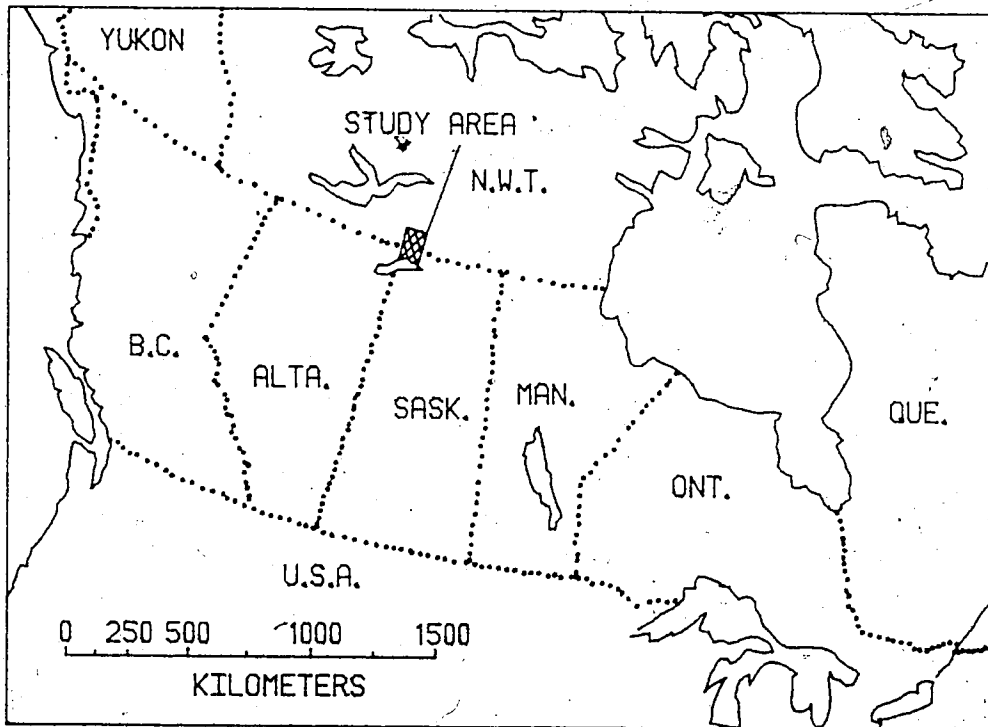


FIG. 1. LOCATION of STUDY AREA

Both these communities may be reached by scheduled passenger

service flights from either Edmonton, Alberta or Prince Albert, Saskatchewan.

The large number of lakes in the area are easily accessible by float plane. Several canoe routes are found in the area, but rapids are common.

Physiography

Rocky hills and ridges, up to 300 feet above lakes and swampy valley flows, rise sharply above the surrounding terrain and characterize most of the surface. Sand plains, ridges, and drift deposits are common in the north, central, and eastern parts where outcrop is scarce and local relief is commonly less.

The map area has been glaciated by an ice sheet moving west-southwest as determined from eskers, glacial striae, and drift cover. Much drift cover is concentrated toward the eastern edge of the map area where sand dunes are active.

The topography has been smoothed by ice movement, however the direction of ice movement was partially controlled by bedrock lithology and structure. In areas of sedimentary rocks, glaciation parallels the bedding, while in gneissic terrain, the direction of foliation controls ice movement direction.

In post glacial times, erosion in the area has been negligible with little deepening or widening of river channels.

Objectives

The objective of this project was to investigate the

extent of granitoid Archean basement in the Hill Island Lake and Tazin Lake areas in the Churchill Province of the Canadian Shield and the possibility of post-Kenoran, pre-Hudsonian events. A further objective was to study the reason why these basement rocks escaped most of the post-2000 ma regional metamorphism and tectonism within the Churchill Province of the Canadian Shield. In addition, an attempt is made to correlate isotopic data with petrographic and structural data on a regional scale.

Previous Work

The area was explored along the Tazin and Taltson Rivers by Charles Camsell, (1916), after J.B. Tyrrell, (1892). Camsell gave the name 'Tazin series' to a group of metasediments intruded by granites and gneisses of a batholith north of Lake Athabasca. F.J. Alcock, (1936), was the first to do systematic reconnaissance mapping and regional geology between the North West Territories boundary and the north shore of Lake Athabasca. He suggested the term 'Tazin group' for the more than one series of early Precambrian sediments and volcanics represented, and mapped the basement as post-Tazin granite, granodiorite, pegmatite, and granite gneisses and gneissic sediments.

Shortly after Wilson (1941), mapped and correlated rock types in the Fort Smith map area with the area north of Lake Athabasca, Henderson (1939), correlated Nonacho group sediments in the Lake Athabasca area, and differentiated granites (gneisses) into 'older' and 'younger'. Later Taylor

in Mulligan and Taylor (1969), while mapping the east half of the Hill Island Lake map area, recognized two types of granite, grey and red. The grey granite was cut locally by the red indicating, in part, an older age. However, the main body of rock of granitic to granodioritic gneisses occur either in sharp contact or gradational contact both along strike and across the dip of foliation. He also recognized two distinct directions of topographic lineaments; one north, the other east with some evidence in the southeast part of the map area of crushed and sheared rocks at the base of linear hills and along valleys, lakes, and streams. The west half of the Hill Island Lake map sheet was covered by Mulligan in Mulligan and Taylor (1969). He has divided the gneissic areas on the basis of amphibolite, schist, and quartzite content either less than or greater than 30%. In the east half of the Hill Island Lake map sheet the change from gneisses to granites is gradational and almost everywhere imperceptible except where crosscutting relationships occur. Mulligan again recognizes two types of granites, grey and red, but refers to their relationship in adjacent map areas.

To the north of the Hill Island Lake map area G.M. Wright (1957), mapped the southeast district of Keewatin on a large scale reconnaissance. The geology of Nonacho Lake and Penylan Lake-Firedrake Lake areas was mapped by Taylor (1959), a couple of years later on a scale of 4 miles to 1 inch. He mapped the oldest rocks in these areas as

sedimentary rocks, mainly quartzite and greywacke or their metamorphosed equivalents, which consist of paragneisses containing quartz and feldspar with lesser amounts of biotite and hornblende. These medium to coarse grained gneisses are light- to dark-grey, poorly- to well-foliated and grade into gneissic granite. They are also locally associated with lit-par-lit gneiss and migmatite. The granitic rock in these areas is of two types: gneissic and massive. The massive granitic rock intrude the gneissic rock and both contain inclusions of the older metasedimentary rock. Grey, well foliated granulite containing tiny clots of red-brown garnet, and blue quartz occurs in the eastern map area and cuts paragneisses and granites. Nonacho group sediments are both cut by and overlie granites in these areas.

To the south of the map area extensive mapping has taken place, especially in the Beaverlodge area, notably by Koster (1961b, 62a, 63b, 65a, 65b, 68b, 70), in the region south of 60° 00' north latitude. Also, Koster and Baadsgaard (1970), reported on the geology and geochronology of the Tazin Lake region. To the south, Christie (1953), and Blake (1955), mapped the region between 59° 45' N and the north shore of Lake Athabasca and 107° 45' W to 108° 45' W. The northern part consists predominantly of post-Tazin granite, granite gneiss, pegmatite and related rocks. To the east of the map area J.W. Hoadley (1955), mapped the Abitau River map sheet on a scale of 4 miles to 1 inch. However, larger

areas adjacent to the Hill Island Lake sheet are unmapped because of glacial overburden and poor outcrop exposure. In spite of the glacial cover, over 9/10ths of the area appears to fall into map unit 2 consisting of grey, pink, and white quartz-feldspar gneiss interbanded with greywacke type rocks or their metamorphosed equivalents from the introduction of much pink granitic rock; and unit 2a consisting of feldspathic quartz-biotite paragneiss.

To the southwest of the map area in the northeast corner of Alberta, Baadsgaard and Godfrey (1972), mapped and dated a Precambrian polymetamorphic complex of igneous, metamorphic, and sedimentary rocks, which have been subjected to granulite facies metamorphism followed by amphibolite facies overprinting by post-2000 ma orogenic events. The rock types now present are massive to foliated, granitoid, granite gneisses, and metasedimentary rocks.

The study area as well as the rest of the Canadian Shield has been studied in terms of metamorphism. In GSC Paper 78-10, Fraser (1978) describes the age and metamorphic grade of rocks in the Churchill Province, District of Mackenzie, for thin section, and previous studies. This study presents a good overall view of the metamorphic evolution of the northwestern Churchill Province.

Geochronology of Surrounding Areas

Geochronology of surrounding areas was reviewed and updated by converting ages in the literature to ages calculated using the newest constants as noted in the

appendix. Geochronology has been done on the area north of Tazin Lake by Koster and Baadsgaard, (1970), and in the Charles - Andrew - Colin Lakes Area, Baadsgaard and Godfrey, (1972). Geochronology has been carried out on a variety of rocks giving 1790 ± 40 ma average ages for K-Ar dates on micas, about 1960 ma from U-Pb whole rock isochrons on the Colin Lake granite-granodiorite series, and 2470 ± 27 ma for Rb-Sr whole rock isochron on pegmatite in granite from the Charles Lake district. A Rb-Sr whole rock isochron on Slave Granite and Arch Lake Granite yields 1944 ± 18 ma (personal communication Baadsgaard). A Rb-Sr whole rock isochron on Fort Chipewyan Granite gives an age of 2319 ± 53 ma (personal communication Baadsgaard).

Money, (1967), using a Rb-Sr whole rock isochron on rocks from the Needle Falls area on the eastern margin of the Wollaston Lake mobile belt, found an age of 1760 ma for meta-arkose, and 2170 ± 70 ma on a best fit isochron. One of four samples belonging to the western granitic rocks is possibly older than 2700 ma. In the Wollaston Lake mobile belt, a Rb-Sr age of 2557 ± 65 ma was determined on the Johnston River batholith by Wanless et al., (1970), and in Money, et al., (1970), Pb/Pb in zircon from the Roper Bay quartz monzonite yields an age of 2405 ma. K-Ar measurements in the area yield apparent ages of 1700 to 1880 ma on micas and hornblende. Using a two-stage model for Pb/Pb mineral isochron, Cumming et al. (1970), obtained an age of 2040 ± 135 ma on a sample of metaconglomeratic hornblende gneiss from

Janice Lake (Pendleton Lake area), in addition to an initial Pb emplacement age of 2530 ± 140 ma. from 7 galenas spread along the belt. A more recent study by Cumming and Scott, (1976), shows old granite having an apparent maximum age of 2614 ma and young granite with an age of 1788 ± 49 ma.

Further work by Coleman, (1970), in the Hanson Lake area of Saskatchewan, part of the stable Flin Flon domain of Lewry and Sibbald, (1977) yields Rb/Sr whole rock ages of at least 2375 ± 30 ma on Amisk-type rocks and granite combined, 2468 ± 60 ma on Amisk-type metavolcanics and 1761 ± 2 ma on cross cutting pegmatitic veins or dykes. The Amisk-type rocks dated are conformable with the surrounding gneisses.

In the Charlebois Lake area, Dragon Krstic, (personal communication) has shown the maximum age of the metamorphosed supracrustals to be about 2300 ma from a Pb/Pb concordia plot.

Near the southwest edge of the Archean stable block Peterman (1962), obtained a single K-Ar hornblende age of 2440 ± 50 ma from the north eastern basement complex north of Nettle Lake.

To the southeast, 30 kilometers north-northwest of Stony Rapids Saskatchewan, a granite cobble conglomerate, dated at 2345 ± 50 ma by K-Ar on hornblende, overlies granitic gneiss dated at 1720 ± 40 ma by K-Ar on biotite. Similarly in the region of Thekulthili Lake a granite cobble conglomerate yields K-Ar apparent ages on muscovite of 2415 ± 50 ma and 2255 ± 50 ma, overlying a hornblende-plagioclase gneiss dated

at 1800 ± 40 ma and 1850 ± 40 ma by K-Ar on biotite according to Burwash and Baadsgaard, (1962). The gneiss was originally metamorphosed at almandine amphibolite facies temperatures and both it and the cobble conglomerate have subsequently undergone greenschist facies metamorphism. Much farther north in the East Arm of Great Slave Lake, similar ages are recorded for intrusive and sedimentary events of 2475 ± 50 ma K-Ar on muscovite on Simpson Island pegmatitic granite intruded by a syenite dyke rock dated at 2200 ± 45 ma K-Ar on biotite. Numerous apparent ages using K-Ar on biotite and muscovite have been obtained by the GSC. In the area of the East Arm with a group of dates from 1750 ± 40 ma to 1845 ± 40 ma in the Fort Smith and Nonacho map areas on gneisses and pegmatite, to 2310 ± 50 ma on granodiorite from just south of the MacDonald Fault, and 2545 ± 50 ma on granodiorite just north of the MacDonald Fault. To the southeast of the East Arm, north of the study area, the GSC obtained a date of 2455 ± 50 ma on paragneiss from Nelson Lake (Sample, GSC 61-82; also Isotopic Age reports of the GSC and GSC Map 1256A).

North of Lake Athabasca, O. Van Breeman in Beck, (1966) obtained two Rb-Sr whole rock ages; one of 1890 ± 100 ma for type-Y younger granite and the other 2285 ± 100 ma for type-O older granite from various localities. Koeppel, (1968) obtained a source age of 2450 ± 50 ma from galena and clausthalite from the Tazin basement of the Beaverlodge area. In the same area Sassano et al., (1972) recorded an

approximate Rb-Sr isochron mineral age of 2250 ma for Donaldson Lake supracrustal gneisses. Also K-Ar dates in the area vary between 1720 ma and 2440 ma.

To the northeast the Hurwitz Group of sedimentary rocks has been dated at 1808 ± 35 ma by Wanless and Eade, (1975), and correlated with the Many Island Lake Group, Munday (1974), and the Thluicho Lake Group, Sibbald et al. (1976).

To summarize these results, post-2000 ma metamorphic ages are most common, but pre-2000 ma apparent ages occur throughout the area with a dozen apparent ages in the range 2200 to 2400 ma. There are a few ages older than this with only three pre-2550 ma apparent ages. These oldest ages occur to the east of the Wollaston Lake mobile belt and close to the MacDonald Fault in the East Arm of Great Slave Lake. This suggests the Archean basement has been reset by numerous local and regional events between 2200 and 2400 ma, after which a post-2000 ma reworking and resetting has taken place in most areas.

B. Geology, Structure and Metamorphism .

General Geology

The regional geology of the area north of Lake Athabasca can be considered on a megascopic scale to represent a stable cratonic platform north of Tazin Lake, known as the northeastern basement complex. This complex consists of a core of mainly granodiorite to diorite as well as aplite to norite compositions. Surrounding this core

zone is a broad zone of migmatite with a similar compositional range. These rocks are fault bounded and appear to be much less affected by a later post-2000 ma metamorphism than the surrounding rocks as shown by Koster and Baadsgaard (1970). These faults curve around from northwest to west and from north to northeast. Similar rocks on the other side of the fault have been strongly reworked by post-2000 ma metamorphism. As has been suggested by Beck (1966), the basement complex to the north may have been rapidly uplifted and shed sediments to the south prior to remobilization in the area. Such an uplift would have raised the platform to near present day levels after two metamorphisms, the first to granulite facies, followed by amphibolite facies regressive metamorphism. The post-2000 ma remobilization could have caused deformation to the point of mylonitization more easily in the less competent sedimentary and metasedimentary belt of rocks to the south, (Christie, 1952). Faulting in the Thainka Lake Area (west half) Koster (1961), has occurred in all rock units, but movement has been confined to the western metasedimentary and volcanic complex as shown by intense folding and dynamic metamorphism with left handed displacement along faults to the north and northwest.

In the Oldman River map area Blake, (1955) points out that the metamorphic grade varies from granulite in the southeast to amphibolite in the northwest with the eastern part of the St. Louis fault as the metamorphic boundary.

This complements Blake's theory that upthrusting of the southern block during mylonitization could have been greater than the normal faulting on the St. Louis fault, so that the rocks in the south represent a deeper crustal level than rocks north of the fault. A study by Beecham, (1970), of the ABC fault and the related Black Bay and St. Louis faults, indicates a left-hand, normal oblique movement for the ABC fault and a slip of 3.7×10^3 m. with the southwest side moving down and southeastward relative to the northeast side.

"Movement on faults in the area imply two main orientations of principal stresses. The orientations apparently occurred at different stages in the uplift of a northeast-southwest elongated dome."

The field relationships show that the NE-SW trending Black Bay and St. Louis fault sets are older than the NW-SE trending ABC fault. Dyke sets in the region can also be used to sort out the ages of different structures.

Koster (1961a, 61b, 62a, 62b, 63, 65a, 65b, 68, 69, 70) has mapped rocks in the field in the area of Saskatchewan below the NWT boundary from the Saskatchewan-Alberta border to the Dardier Lake W1/2 107° 45' W. De Zoysa (1974), has also mapped rocks in the west half of the Ena Lake area. The synthesis of the geology of these regions can be summed up in the following subdivision: Martin Formation, Granodiorite-Diorite Series (Northeastern Basement Complex), and Paragneisses. The paragneisses can be correlated across the Tazin River fault and across the map areas concerned.

However, the gneisses vary in degree of homogenization and migmatization. According to Koster (1970),

"the isoclinal folding of the gneisses predates anatexis; in many places detail folding is more or less obliterated by homogenization of the gneiss"

Further, Koster (1970), claims

"the granodiorite diorite series is of anatectic origin and possibly syntectonic to late tectonic. Partly fragmented linear basic dykes in the center of the composite part of the pluton indicate profound remobilization of the series.

Mylonitization took place before intrusion of late tectonic Kenoran granite."

In addition to the two main map units, the area has been cut by mafelsic and mafic dykes and felsic veins. These northwesterly trending dykes and veins have been correlated with similar dykes described from the Slave province. The dykes appear to vary in age, but can be correlated with the swarm of orientations recorded in Stockwell et al. (1970).

On the eastern edge of the Wollaston Lake mobile belt Money (1965), (1966), in the Needle Falls area, recognized inclusions of the assemblage hornblende-hypersthene-plagioclase-quartz of the hornblende granulite subfacies and also in the Pederson Lake complex in the Daly Lake area an assemblage of hypersthene-hornblende-plagioclase-quartz-(K-feldspar)-(biotite). In this complex the biotite in both basic (hypersthene amphibolite) and acidic rocks

(charnockite) and at least some of the hornblende in the acidic rocks are products of retrograde metamorphism. Within the Wollaston Lake mobile belt itself, the highest grade of rocks reported are amphibolite facies. This difference in metamorphic grade is explicable in terms of an Archean granulite facies basement overprinted and incompletely retrogressed by amphibolite facies post-2000 ma metamorphism. Lewry and Sibbald, (1977) suggest that the Archean inliers in the eastern part of the Wollaston domain were emplaced as gneiss domes during post-2000 ma remobilization of the Archean basement.

The geology of the Hill Island Lake map area (see map 2) appears to be similar to the geology immediately to the north of Lake Athabasca. The main body of rocks, called the Nolan Granodiorite, is composed of leucocratic biotite granite to hornblende biotite granodiorite and associated gneisses, with pegmatite, some diorite and quartz diorite, and minor diabase dykes. The rocks vary in color from light- to dark- grey, to pink, and vary from very fine to coarse grained. Most rocks have a gneissose texture with augen of K-feldspar common, while others have a massive to granoblastic to porphyroblastic texture in hand specimen with occasional schistose texture. Two main directions of foliation were observed in the field; a north-south vertical foliation, and a northeast-southwest vertical to steep northwesterly dipping foliation.

The sample locations are roughly on a grid system with

about 15 kilometer spacing, as sampling was done by float plane. The sampling took place north of 60° 00' north latitude up to 60° 40' north latitude, and from 108° 00' west longitude to 109° 38' west longitude, and covers an area of about 5000 square kilometers.

Structure, Magnetism and Metamorphism

Two main foliation directions were observed in the field. On topographic and geologic maps of the area, the structural trend follows a U-shape which closes to the south and is open to the northeast. However, to the north of the sampled area, three main foliation directions appear from the geologic, topographic, and aeromagnetic maps (see map 1 in pocket). In the northwest corner, the dominant foliation is northwest, while in the north-central region, it is east southeast, and in the northeast corner, it changes abruptly to a northeast trend.

The shaded area in map 1, 3500+ gammas, depicts areas of positive magnetic relief representing more mafic rocks. Granulite facies rocks also appear as areas of positive magnetic relief. The elliptical shaped body north of Tazin Lake outlines the change from Koster's granodiorite I to granodiorite II. This is prominent because of the abundance of granites and aplonites intruded into the granodiorite II. The shaded area is close to or covers locations 6010, 6022, and 6023. Other areas of aeromagnetic high include south of Tazin Lake in a belt curving up through the southeast corner of the area including locations 6011, 6025,

and 6033. This area south of Tazin Lake represents granulite facies rocks which appear to trend parallel to the magnetic anomaly. A large area of magnetic high in the north central region lies alongside the remobilized zone which trends northeast. Mylonite zones tend to show up as magnetic lows. A second area of magnetic high lying parallel to the first northeast trending high may be separated by a mylonite belt or simply a different rock type. From the samples in these areas it appears as if a mylonite belt runs between them. The aeromagnetic high in the northeast corner suggests that the unmetamorphosed Archean basement may continue to the northeast.

Although structural field relationships have not shown which foliation is primary and which is secondary, thin section work and structural relationships south of 60° north latitude indicate that the strong northeasterly trend is secondary and related to shearing stress as evidenced by mylonitization seen in thin section. In fact, the bright pink map unit on the map of Hill Island Lake, (Mulligan and Taylor, 1969), named feldspar porphyry, corresponds very well with samples showing cataclasis. These rocks were aligned northeast-southwest and this structural lineament direction may be considered secondary, post-orogenic, and post-metamorphic. The other foliation direction, north-south, may be considered older. However, it may be possible that there is more than one northeast-southwest foliation. In the Burchnell Lake area, mafesic to mafic

dykes have been metamorphosed to granulite facies conditions, followed by a remobilization, recrystallization, and development of a new foliation and lineation. The foliation strikes north-northwest truncating dykes and dyke fragments. This relationship suggests that the north-south foliation occurred after amphibolite facies retrograde metamorphism. Also, a southeast striking dyke of porphyritic metadiorite that has been locally mylonitized has been offset righthandedly by a fault striking northeast. The dyke had undergone granulite facies metamorphism and been retrograded. This suggests that a northwest-southeast compression associated with a northeast foliation occurred prior to granulite facies metamorphism in the late Kenoran. Along the southern edge of the Hill Island Lake map sheet, an east-west striking diabase dyke cuts biotite granitic gneiss. The gneiss, which has a north-south vertical foliation and is granoporphroblastic to mylonitic in texture (see plate II. a.), has undergone both granulite facies and retrograde amphibolite facies metamorphism followed by shearing along a north-south alignment. The dyke rock is physically undeformed, but has some alteration of hornblende to biotite and carbonate, and plagioclase to epidote. The K-Ar whole rock age on the dyke is 1930 ± 40 ma as shown in the results.

On the gravity map of the area, Series No. 124, Bouguer anomalies yield low readings of -600 to -500 milligals, relative to the surrounding region. These low readings

represent less dense felsic rocks at about 5 to 10 kilometers depth. Farther to the northeast in the Penylan-Firedrake map area, (Taylor, 1959), Gravity Map Series No. 125, more mafic rocks give readings of -400 milligals. Directly north of the map area in the region of Alcantara Lake, a low of -600 milligals occurs. Still farther north between Doran Lake and Gray Lake, two lows of -750 milligals occur. This suggests an extensive area of thick sedimentary rocks.

The Archean rocks in the Hill Island Lake and Tazin Lake areas have undergone a period of granulite facies metamorphism in late Kenoran times. Although hypersthene was not recognized in thin section in the Hill Island Lake area, a number of other indicators of granulite facies metamorphic conditions are present. These indicators are the orthoclase perthite, antiperthite, the greenish-brown to brown color of hornblende, corroded zircons, tschermakitic hornblende, and the presence of relict pyroxene grains. These rocks were then retrograded to amphibolite facies conditions with slow cooling as evidenced by relict pyroxene, the anorthite content of plagioclase ($An \geq 17$), the presence of epidote, and the presence of tschermakitic amphibole. This retrograde metamorphism took place at a depth of no more than 20 kilometers, as evidenced by lack of muscovite, the presence of K-feldspar in most samples, and the average apparent age of hornblende (2460 ± 90 ma) as discussed below.

C. The Retention of Radiogenic Argon by minerals

Although potassium argon dating may be straightforward, representing the time of crystallization of a mineral, this is not always the case. A number of factors can 'reset' the potassium argon clock by allowing radiogenic argon to escape from the lattice of the mineral grain being measured or by allowing 'excess' radiogenic argon into the lattice.

Factors which affect closure of the lattice to gain or loss of argon are: grain size, excess partial pressure of radiogenic argon in the whole rock, later metamorphism, deformation, varying rates of uplift, diffusion of argon at high temperature, diffusion due to lattice disordering, and diffusion due to the presence of water.

Grain size has an effect on argon loss by greater loss of argon at and near the surface of the mineral grain if the grain size diameter is < 50 microns. Smaller grains therefore have a greater portion of surface argon loss. In this project, the effect of grain size has been minimized by measuring mineral separates of a standard grain size (600 to 150 microns).

During a strong heating event, argon is lost from the mineral lattices. If the argon does not diffuse out of the rock before lattice closure, there may be an excess partial pressure of argon. This will cause incorporation of excess argon into lattices which stabilize at relatively low temperatures such as biotite.

Later metamorphisms may cause either argon loss or gain

by opening the mineral lattice at high temperature. In this case the temperature of metamorphism is important because different mineral lattices close off argon diffusion at different temperatures (biotite and muscovite normally close at much lower temperatures than hornblende). A metamorphism can therefore reset the K-Ar date of biotite without resetting that for hornblende, or it can partially reset the K-Ar date of a mineral if the temperature is at or near the closing temperature.

Deformation by shearing stress can temporarily dislocate mineral lattices causing argon loss. Particularly susceptible to this kind of dislocation is biotite, although deformation also affects hornblende's argon retention.

The rate of uplift in conjunction with the geothermal gradient affects argon closure directly by setting rock temperature at depth. Therefore, rapid closure to argon loss can be effected by rapid uplift and accompanying temperature drop. By the same token a lower temperature of argon closure accompanies slow uplift and cooling. A study by Dodson, (1973), found that closure temperature, the temperature at the time corresponding to the apparent age, depends on diffusion size, geometry, and cooling rate. For a biotite crystal with an activation energy of 21 Kcal/mole and diffusion rate of $2 \times 10^{-10} \text{ s}^{-1}$ at 600°C assuming diffusion only along basal cleavage planes, and a cooling rate of 100°C/my. , the closure temperature would be 222°C . The closure temperature of Rb/Sr in an Alpine biotite is 300°C .

if the cooling time is 10 my. For a cooling time of 20 my. the closure temperature is 280°C.

Diffusion of argon from mineral lattices at high temperature would not normally be important because of the time factor involved. However, according to Damon (1968), complete argon loss by diffusion in an amphibole could be achieved in 600,000 years at a temperature of 475°C based on the work of Evernden and Hart. This means that complete argon loss could easily have taken place in amphiboles even at amphibolite metamorphic grade temperatures over several millions of years. On the other hand, Gerling, et al., (1965), found that the activation energy for argon loss from 5 amphiboles varied from 110 to 200 kcal/mole, decreasing systematically with increasing iron content. They calculated a minimum temperature required to cause significant (0.90%) argon loss in 10^8 years and found a range of 470°C to 670°C again depending on iron content.

In conjunction with the other factors mentioned, diffusion can take place more readily from a disordered lattice under the same conditions. Lattice disordering relates to the proximity to the size of the unit cell. This means that a unit cell of hornblende close to the ideal size will be close to 100% ordered. As the cell size changes from ideal, the lattice becomes more disordered. How chemical composition affects argon retentivity has been investigated by Gerling et al. (1965), and for calcic amphiboles by O'Nions et al. (1969), and O'Nions (1969). The argon

retentivity does depend on chemical composition if the lattice is disordered. It has been found that disordered amphiboles with a higher proportion of weaker bonding cations in the M1, M2, and M3 sites, are less retentive of argon. The most common weaker bonding cation is $2+Fe$. This is based on the theory that cations with weaker ionic bonds will leave larger spaces between bonds for argon to pass through when the lattice is heated. This finding was later confirmed by Evans and Lambert (1974). Therefore a more iron-rich tschermakitic hornblende would be expected to close its lattice to argon loss at a lower temperature, yielding a younger potassium argon age than a magnesium rich sample. In fact O'Nions et al. (1969) suggest that iron rich hornblende may close to argon loss during slow cooling at roughly the same temperature as mica because argon diffusion will be controlled by the diffusion rate. However, during updating the diffusion of argon will be controlled by activation energy which in iron rich hornblende is much higher than that for micas. In this case disordering is expected along with a spread in hornblende apparent ages due to differences in proportion of iron content.

In addition, diffusion of argon from a mineral lattice may be affected by the action of water in chemical weathering and alteration and changes in the potassium content (Faure, 1977). Since this area has undergone granulite facies metamorphism the rocks were dewatered except in fault zones and younger metasedimentary rocks.

II. Results and Interpretations

A. Results

Introduction

From the 37 sample locations visited, a total of 57 apparent ages were obtained from 49 rock samples. The apparent ages were obtained for 15 amphibole, 1 whole rock, 1 muscovite, and 40 biotite ages. Some ages, however, are unusable due to the nature of the sampled material, which caused these samples to be minima for K-Ar dating (see Plate V. b.).

The microprobe results from the amphiboles were used to calculate biotite corrected compositions for these amphiboles.

In the amphibole samples, the major contaminant is biotite. However, crushing the samples to a finer grain size to remove biotite would not have succeeded, since the biotite formed microintergrowths, averaging 5 to 10 microns in length, within the amphibole. This also posed problems when physical separation techniques were applied to the sample.

To overcome this physical separation problem, grain mounts of amphiboles were prepared for analysis using energy dispersive microbeam analysis. The corrected potassium value for the amphibole was then used to find the proportion of contaminant and to correct for the argon values measured in the contaminated samples.

Table 1 Potassium Argon data for biotite (B), muscovite (M), and whole rock (W), from the Hill Island Lake Area, N.W.T.

Sample	40K(ppm)	40Ar (ppm)	40Ar/40K	40Ar/40Ar Total	Date ma
6000 B	8.43*	2.310	0.274	0.976	2320
6001 B	8.83	1.812	0.205	0.984	1960
6003-A B	7.42*	1.502	0.202	0.980	1940
6004 B	7.98*	1.986	0.249	0.997	2190
6005-A B	8.57*	1.948	0.227	0.989	2080
6005-B B	8.63*	1.829	0.212	0.976	2000
6005-C B	8.44	1.916	0.227	0.989	2080
6005-D B	6.55*	1.406	0.215	0.970	2010
6006 B	7.63	1.384	0.181	0.991	1810
6007 B	6.94	1.592	0.228	0.986	2090
6008 B	5.85	1.386	0.237	0.993	2130
6010-A B	7.01*	1.911	0.273	0.977	2310
6010-A? B	6.55*	1.865	0.284	0.965	2370
6010-B W	2.19*	0.438	0.201	0.972	1930
6011 B	1.50*	0.306	0.169	0.957	1730
6012 B	8.36	1.643	0.197	0.989	1910
6013-A B	7.36	1.688	0.229	0.989	2090
6013-B B	8.33	2.079	0.250	0.990	2200
6014 B	7.87	1.532	0.195	0.998	1890
6015 B	7.75	1.930	0.249	0.993	2190
6016 B	9.04	2.098	0.232	0.990	2110

Table 1 (cont.)

Sample	40K (ppm)	40Ar (ppm)	40Ar/40K	40Ar/40Ar Total	Date ma
6017 B	4.78	1.044	0.219	0.997	2030
6018 B	9.52	2.469	0.259	0.993	2250
6020 B	7.62	1.898	0.249	0.996	2200
6021 B	7.28	1.792	0.246	0.986	2180
6022 B	8.42	2.248	0.267	0.994	2280
6023-A B	6.94	1.854	0.267	0.990	2280
6023-B B	7.05	1.817	0.258	0.961	2240
6025 B	8.03*	1.558*	0.194	0.991	1890
6026 B	6.67	1.250	0.187	0.986	1850
6026 M	10.24	2.087	0.204	0.994	1950
6027-B B	7.53	1.899	0.252	0.987	2210
6028-A B	7.11	1.781	0.250	0.982	2200
6028-B B	7.37	1.778	0.241	0.980	2150
6029 B	5.32	1.298	0.244	0.981	2170
6030 B	7.69*	1.429	0.186	0.633*	1840
6031 B	8.03	1.631	0.203	0.998	1940
6032 B	7.34	1.788	0.244	0.999	2170
6033 B	1.40	0.293	0.209	0.910	1980
6034 B	8.18*	2.073	0.253	0.993	2220
6035 B	8.57	2.283	0.267	0.988	2280
6036-A B	4.05	1.039	0.257	0.961	2230

*sample poor, or analysis poor

Table 2 Potassium Argon data for hornblende from the Hill
Island Lake Area, N.W.T.

Sample	40K (ppm)	40Ar (ppm)	40Ar/40K	40Ar/40Ar Total	Date ma
6001	1.599	0.473	0.296	0.967	2420
6003-B	1.036	0.356	0.344	0.964	2620
6003-C	1.012	0.312	0.308	0.905	2480
6005-A	1.706	0.468	0.275	0.976	2320
6005-C	1.273	0.381	0.299	0.985	2440
6013-B	1.739	0.468	0.268	0.981	2290
6015	1.587	0.488	0.307	0.716	2470
6020	1.249	0.364	0.291	0.983	2400
6022	1.429	0.427	0.299	0.958	2430
6025	0.975	0.156	0.223	0.979	2060
6028-A	1.747	0.519	0.297	0.974	2430
6028-B	1.164	0.396	0.340	0.970	2610
6032	1.663	0.472	0.284	0.974	2370
6034	1.590	0.435	0.273	0.970	2320
6036-A	1.006	0.313	0.302	0.910	2450

Table 3 Composition Correction For Amphiboles

Sample	40K (ppm)	40Ar (ppm)	40Ar/40K	Date ma
6001	1.363	0.424	0.311	2490
6003-B	1.140	0.390	0.344	2620
6003-C	1.023	0.314	0.308	2480
6005-A	1.337	0.383	0.286	2380
6005-C	1.222	0.370	0.303	2450
6013-B	1.673	0.451	0.269	2300
6015	1.606	0.494	0.307	2470
6020*	0.677	0.221	0.326	2550
6022	1.398	0.418	0.299	2430
6028-A	1.703	0.507	0.298	2430
6028-B	1.253	0.425	0.340	2610
6032	1.382	0.405	0.293	2410
6034	1.731	0.472	0.273	2320
6036-A	0.855	0.274	0.321	2530
6025**	0.65	0.156	0.240	2150

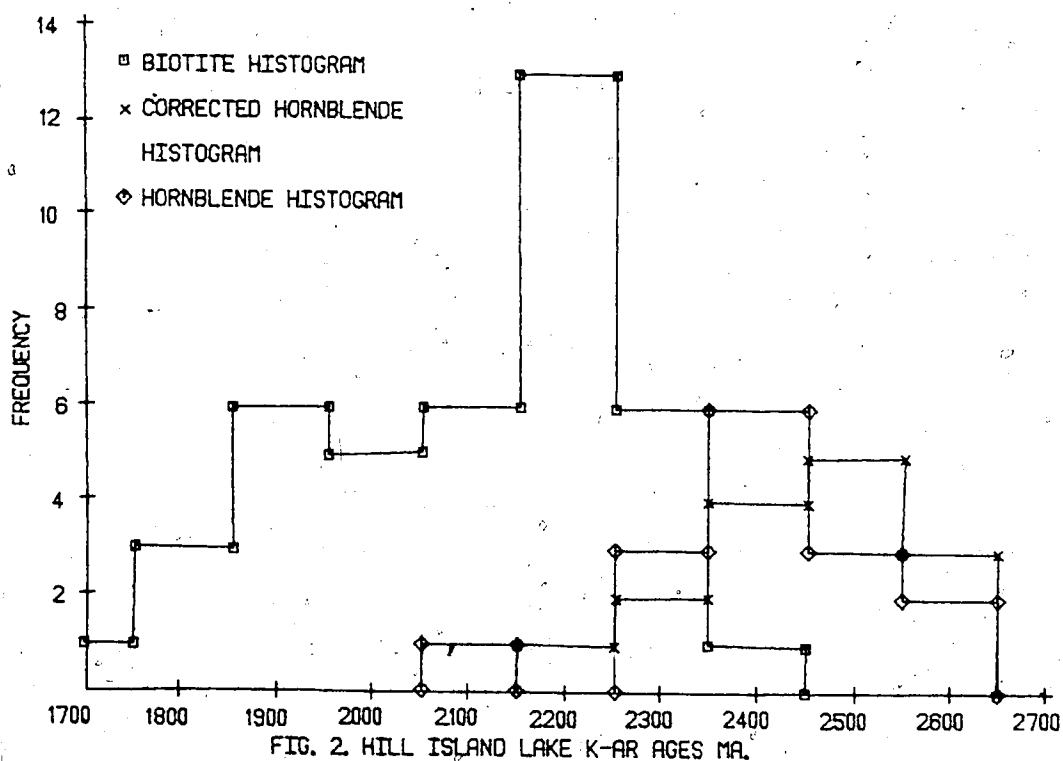
*two amphiboles in this sample; dark green and light green;
sample probably not homogeneous

**correction was made by estimating proportion of
biotite in amphibole from thin section.

B. Interpretations

Review of all new age data

Potassium argon apparent ages for biotite and hornblende from tables 1, 2 and 3 can be interpreted in histogram plots. Figures 2, 3 and 4 are histogram plots of Hill Island Lake K-Ar ages in 100 my. intervals, Hill Island Lake



K-Ar ages in 50 my. intervals, and a combination of Hill Island Lake and Tazin Lake K-Ar ages in 100 my. intervals respectively. In figures 2, 3 and 4 the hornblende age distribution begins at 2600 ma. This may correspond to a Rb-Sr whole rock isochron age of 2620 ± 90 ma on country rock from the Tazin Lake area. Figures 2

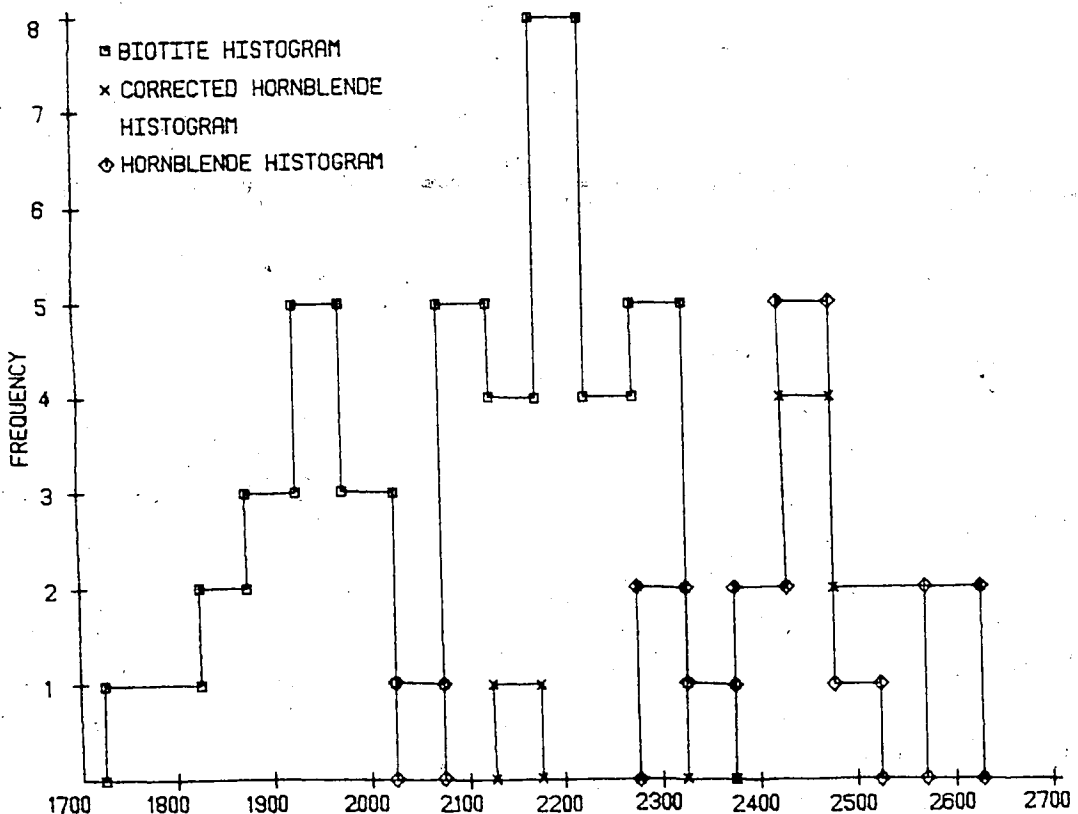


FIG. 3. HILL ISLAND LAKE K-AR AGES MA.

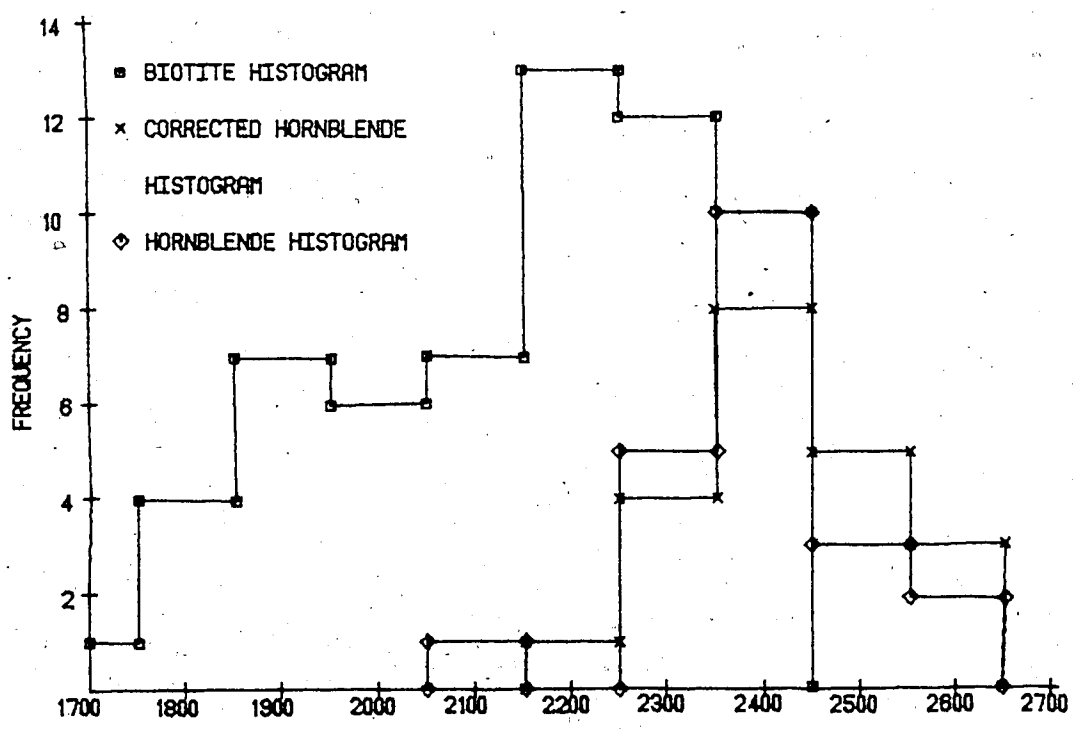


FIG. 4. HILL ISLAND LAKE AND TAZIN LAKE K-AR AGES MA.

and 3 indicate a frequency peak at 2400 ma and 2450 ma respectively for hornblende, and 2500 ma and 2450 ma for corrected hornblende respectively. This corresponds to the Rb-Sr whole rock isochron age of 2533 ± 15 ma on the granite-granodiorite series to the north of Tazin Lake. Corrected hornblende refers to hornblende apparent ages calculated from microprobe potassium results to correct for biotite contamination. The frequency peak for hornblende in figure 4 occurs at 2400 ma. At the same time the biotite distribution rises strongly at 2400 ma and peaks at 2300 ma. This corresponds to the Rb-Sr isochron age of late pegmatite intrusions in the Tazin Lake area at 2338 ± 25 ma. In figures 2 and 3, the biotite age distribution also starts at 2400 ma and 2350 ma, however the first biotite age peak occurs at 2200 ma. This first biotite age peak may represent a metamorphic event before 2200 ma or simply a cooling with uplift through the blocking temperature of biotite since there is about 300 my. between the hornblende peak and the first biotite peak. Also, this peak is not sharp but the distribution tails off on either side. A second biotite distribution peak occurs at 1900 ma, 1950 ma and 1900 ma in figures 2, 3 and 4 respectively. This may correspond to a 1960 ma U-Pb whole rock isochron age for intrusives from northeast Alberta. It may also correspond to a 1930 ma K-Ar age on a diabase dyke from location 6010. Figure 3 accentuates the biotite

distribution peak at 1950 ma but is not very significant because the error in K-Ar ages is ± 45 my., while the age interval is 50 my., or 1 sigma confidence. If a histogram is plotted using 20 my. age intervals, it will be meaningless because the confidence for this interval is about 30% and the sample size n is much too small to have any significance as there are 45 intervals for 57 apparent ages.

To test whether or not excess argon has been incorporated into the biotite lattice, biotite age versus hornblende age was plotted in figure 5. This plot shows a lack of correlation between biotite and hornblende ages indicating no incorporation of excess argon into the biotite lattice. This noncorrelation is supported by the fact that no K-Ar ages are in excess of the maximum Rb-Sr ages in this area. Also, the geographical distribution in figure 6 and map 1 in the pocket, shows a pattern of biotite ages as opposed to hornblende ages.

Biotite Ages

The biotite apparent ages which are represented in figure 6 and map 1 by age contours, display a plateau like area or inlier of preserved older rock extending northeast. The southern end of this plateau region contains a region of 2300+ ma up to 2450 ma biotite ages. This corresponds to the average K-Ar age of 2360 ± 40 ma of rock from the Tazin Lake area. All the

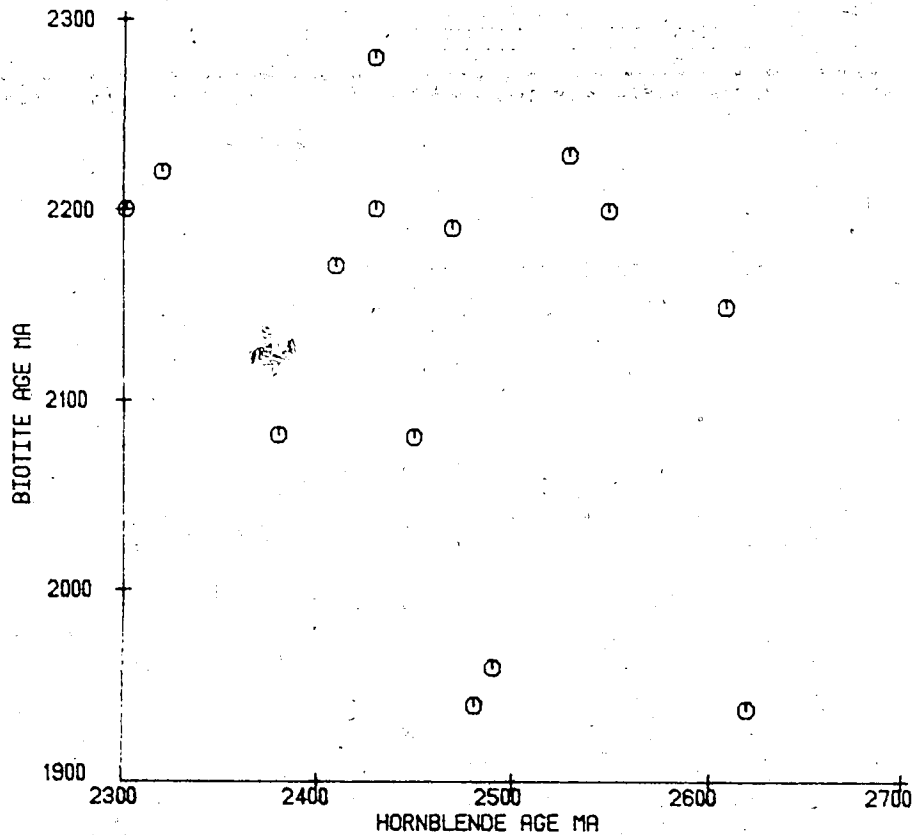


FIG. 5. BIOTITE APPARENT AGE VS. HORNBLENDE APPARENT AGE.

2300+ ma apparent ages in this area, fall within a circular structural region which defines the boundary between granodiorite I and granodiorite II in the area north of Tazin Lake, as outlined by 3500+ gammas. This suggests a geologic event and more rapid uplift for this particular region, as hornblende ages in this area are not older than biotite ages and biotite ages are older here than in the rest of the inlier.

Biotite age contours indicate post-2000 ma resetting along the margins of the inlier. The biotite

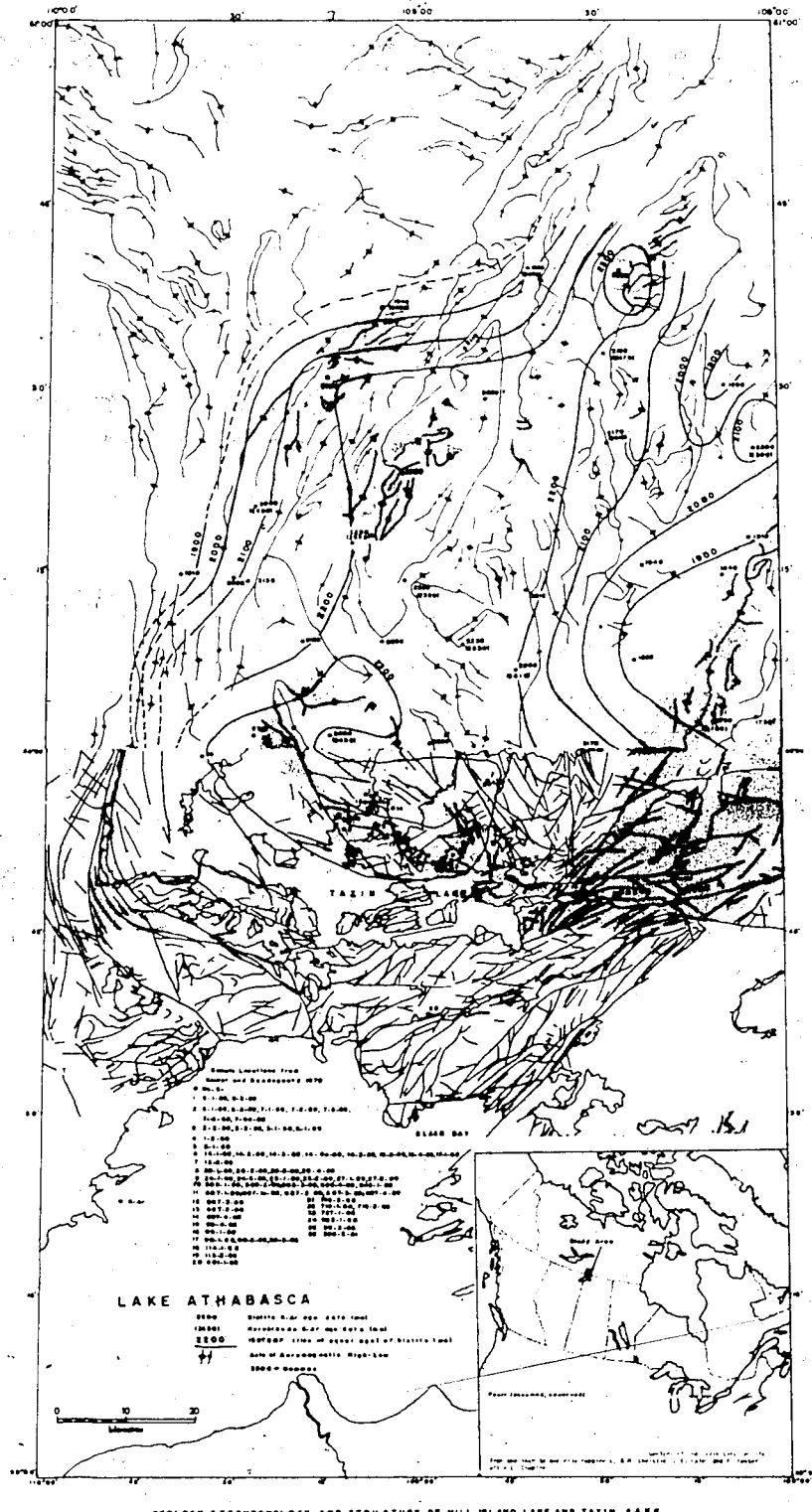


FIG. 6. GEOLOGY, GECHRONOLOGY, AND STRUCTURE OF HILL ISLAND LAKE TAZIN LAKE AREAS

age contours are very close together in the west as they approach the Tazin River and Hill Island Lake. This region contains mixed granites, gneisses and metasediments strongly reworked and remobilized during post-2000 ma events. Along the northern edge of the sample area this sharp drop in age contours is also seen and appears to represent post-2000 ma remobilization, as a fault zone appears to run northeast along the plateau margin. The eastern edge of the plateau is not distinct as biotite age contours gradually decrease to 1800 ma. This suggests that a post-1900 ma thermal pulse has variably reset the biotite ages. The inlier has also been cut by faults of various ages of which location 6014 must be near a post-2000 ma fault, striking northeast.

Hornblende Ages

Results from 15 hornblendes are shown in Tables 2 and 3. Table 2 reports hornblende ages from the Hill Island Lake area. Table 3 uses the same data in combination with microprobe K values from Table 5 in the appendix and Table 1, to correct for biotite contamination. This microintergrowth of biotite is characteristic of tschermakite, (Schrocke, 1976) which may occur as a result of retrograding from granulite facies metamorphic conditions to a lower metamorphic grade. Evidence of biotite microintergrowth in amphibole is seen in thin section (see Plates I., II., III.a., IV.

and VI.a.). Contamination correction is calculated by finding the difference in ppm 40K between isotope dilution and microprobe results. The portion of 40K remaining is assumed to represent biotite. To correct for 40Ar contamination by the same biotite, the 40K excess is multiplied by 40Ar/40K ratio for biotite from the same rock. The resulting excess 40Ar value is then subtracted from the 40Ar value obtained for hornblende and the resulting corrected 40Ar/40K yields a biotite corrected age.

Sample 6020 contains both a light green and a dark green amphibole. Because of the small amount of sample used for microprobe grain mounts (about 50 grains), the sample is inhomogeneous. This means the potassium values may not correspond to the argon values. Sample 6025 was not available for grain mounting, so a visual estimate of biotite content was made from thin section (see plate IV. b.).

The corrected amphibole ages show a wide spread of K-Ar dates ranging from 2620 ± 50 ma to 2150 ± 45 ma with an average age of 2460 ± 95 ma. The amphibole ages not corrected for biotite show a similar spread of dates with an average age of 2430 ± 95 ma. This spread of ages is similar to biotite, but does not seem to relate to geographical distribution as biotite does. This is emphasized by the fact that different hornblende samples from the same location eg. (6003-B, 6003-C),

(6005-A,6005-C) and (6028-A,6028-B), indicate widely varying ages using both Table 2's and Table 3's results. However, in the southern end of the inlier the maximum hornblende apparent age is 2430 ma. This suggests that the resetting event in the south end of the inlier was stronger than the rest of the inlier. Along the margins of the inlier hornblende apparent ages are older than biotite apparent ages by as much as 700 my. This again suggests post-2000 ma events which reset biotite.

If the age of amphibolite facies retrograde metamorphism is 2400 ma to 2450 ma, then hornblende may have outgassed argon during a 2250 ma to 2200 ma regional metamorphism or simple closure upon cooling through the closing temperature. The important question for biotite contamination correction is whether or not the hornblende remained closed to outgassing of argon from biotite inclusions at 2200 ma to 2250 ma. The correction table, Table 3, assumes that the argon from biotite inclusions in hornblende was outgassed at 2200 ma to 2250 ma, as most biotite occurs along cleavage planes. If the argon was not outgassed at this time, then the microprobe correction does not apply and the original results stand. A third possibility is partial outgassing of biotite argon at 2200 ma to 2250 ma with an intermediate age resulting. In addition Table 3 uses the potassium values from the microprobe which do not include the average of the total hornblende grain, but

exclude biotite, and other inclusions such as quartz, epidote and magnetite. This means the microprobe potassium value will be higher than the corresponding flame photometer potassium value, if biotite is not present. Therefore, it is possible that the corrected tables yield low Ar/K values and low ages.

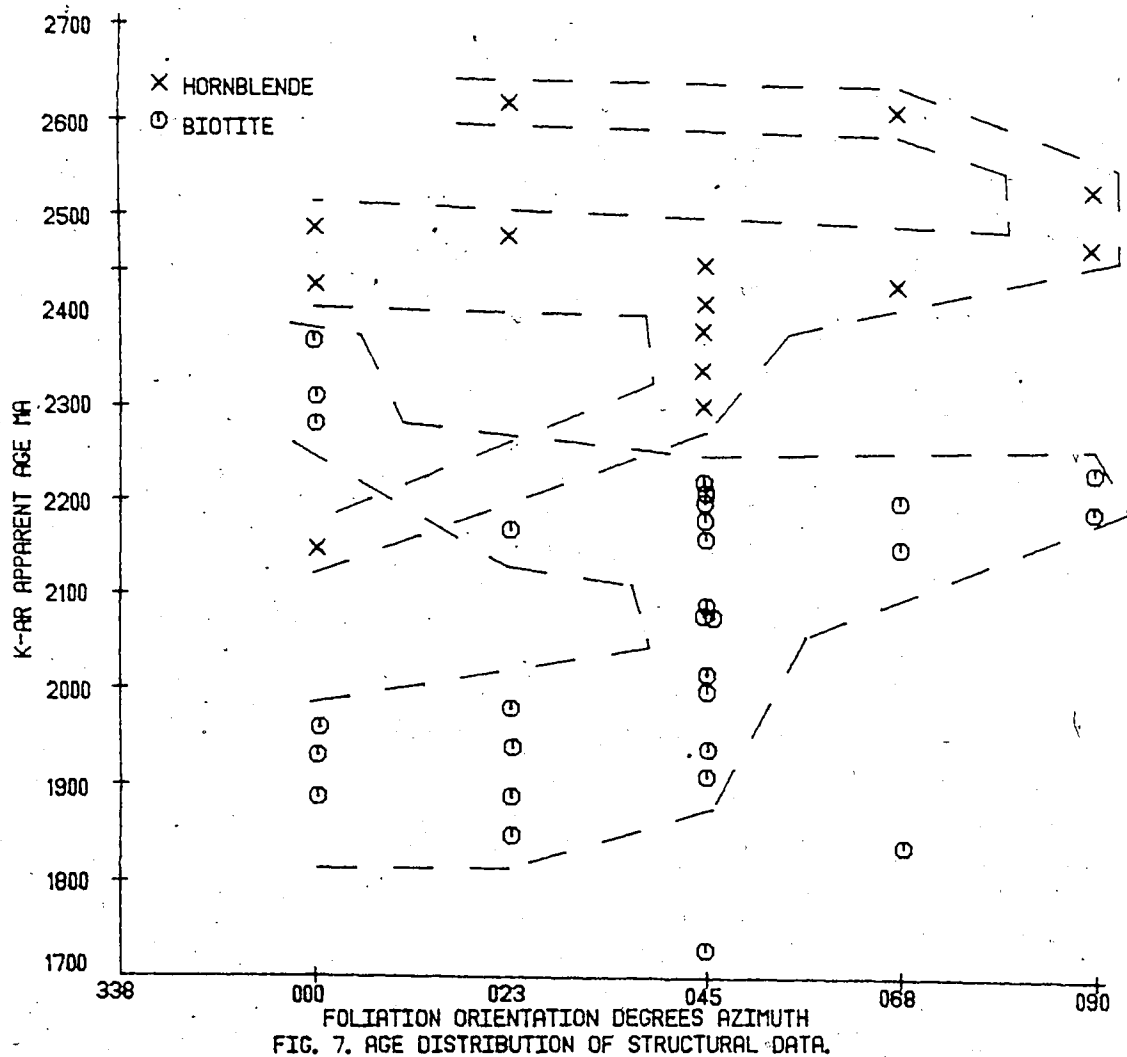
These results also suggest that hornblende from the Tazin Lake area may be contaminated by biotite as seen in plate IV.a. of sample 6022, a massive hornblende biotite granite belonging to Koster's granodiorite II complex. If this is the case, the hornblende ages will not get significantly older or younger because they have been contaminated by biotite of approximately the same age.

General Metamorphic and Igneous History

When the field relationships are compared to K-Ar apparent ages, a rough picture of the metamorphic and igneous history appears. Near the southern edge of the Hill Island Lake area at location 6010, a diabase dyke cuts through granitic gneiss as described previously. The K-Ar whole rock age on the dyke (probably a minimum age) is 1930 ± 40 ma. This age is a minimum because the whole rock contains plagioclase which loses its argon readily. These rocks are close (15-20km) to the Hill Island Lake belt of metasedimentary rocks, which have been strongly reworked by post-2000 ma events. A massive hornblende diorite, sample 6036, is cut by a one-meter

wide north-south vertical dyke of hololeucocratic granite. The biotite K-Ar apparent age of the diorite is 2235 ± 45 ma, while the hornblende K-Ar apparent age is 2525 ± 50 ma. This dyke rock is physically undeformed, but altered: plagioclase to sericite and carbonate, biotite to chlorite.

When the foliation directions of the Hill Island Lake area rocks are compared with the K-Ar apparent mineral ages derived, a rough picture of the sequence of tectonic events appears (see figure 7). The oldest rocks contain a north-south vertical foliation associated with granulite facies metamorphism. From rocks that are only slightly younger, a weak west-south-west foliation dipping moderately to the north appears. This may be related to the Tazin River fault and hinged uplift or doming at the time of amphibolite facies retrograde metamorphism. Following this, the ~~compression~~ direction gradually changes from northwest-southeast to east-west by 1930 ma, resulting in a change of foliation direction from northeast-southwest to north-south. Although the results from figure 7 have been variably affected by post-2000 ma metamorphism, a sequence of events of a particular tectonic style was deduced. Further, some of these rocks have undergone weak metamorphism associated with shearing deformation. The main shearing deformation appears to be associated with 1800 to 2200 ma tectonism and is a late stage event in the area.



The lack of aluminous metamorphic minerals in the area, such as sillimanite, cordierite, and garnet is due to the lack of excess alumina in the rocks. From the point of view of provenance, this lack of excess alumina suggests igneous source material for most of these rocks, except some biotite schists found on the east side of the map area.

Using the apparent age of hornblende and the blocking temperature of average hornblende, about 550°C, the time of amphibolite facies retrograde metamorphism,

2460±90 ma is obtained. There are a few older hornblende apparent ages from more magnesium-rich hornblendes as shown below, that represent higher temperature granulite facies conditions. Different hornblendes from the same location give different ages due to compositional differences. This difference in ages may be caused by a secondary thermal event at amphibolite facies temperature or simply by climatic uplift and cooling from granulite facies conditions. The wide spread of both hornblende and biotite ages suggest a deep burial at the time of granulite facies metamorphism, followed by slow uplift and cooling as is the case in the Scottish Caledonides, (Dewey and Pankhurst, 1970). Using a minimum geothermal gradient of 30°C/kilometer and a granulite facies temperature of 750°C, a maximum depth of 25 kilometers is obtained. The rocks were uplifted to a maximum depth of about 18 kilometers at the time of amphibolite facies retrograde metamorphism in the main body of the inlier. At the time of late pegmatite intrusion in the Tazin Lake area the south end of the inlier had been uplifted to a maximum depth of 6 kilometers and possibly 3 kilometers since most of the biotites are older than the Rb-Sr pegmatite isochron age. However, hornblendes had closed to argon loss while almost no biotites record this event. This heating event was not as strong in the main body of the inlier since most hornblende ages appear to have escaped resetting.

A later heating event may have occurred between 2200 and 2250 ma at which time biotite K-Ar ages are set. Events which may correlate with this resetting and uplift are: 2338 ± 25 ma Rb-Sr pegmatite intrusions near Tazin Lake, the age of Beck's older granite at 2280 ± 100 ma, the age of Donaldson Lake supracrustal gneisses at about 2250 ma, the age of Charlebois Lake supracrustals at about 2300 ma, the age of Fort Chipewyan granite at 2319 ± 53 ma, and the K-Ar apparent ages of granite cobble conglomerate in the Thekulthili Lake area and in the Stony Rapids area. Hornblende ages appear not to be reset so that a heating event at this time would not be very strong. This is shown by the fact that biotite ages in the Tazin Lake area have not been reset at this time. This lack of 2200 ma biotite apparent ages in the Tazin Lake area, also indicates that these rocks were at a high level in the crust at this time, and were relatively cool.

Post 2000 ma tectonism appears to have cut through the inlier along the northwestern edge where biotite apparent ages are 1940 and 1960 ma, and in the northeast where biotite was reset at 1890 ma. This correlates well with intrusive activity to the southwest and south, north of Lake Athabasca. By the time of strong 1800 ma heating and remobilization, the present day surface rocks were at or near the surface, so that heating only reset biotite ages along the margins of the inlier. One

hornblende apparent age from location 6025 was also partially reset.

Hornblende Composition

Table 5 in the appendix is a compilation of the microprobe results which are used to find the composition of amphiboles. It is found that the amphiboles are calcium amphiboles and fall under the general heading of amphiboles which includes common hornblende, tschermakite, edenite, and pargasite. Since the microprobe determines total iron, the sample formulas have all been calculated on the assumption of 80% 2+Fe and 20% 3+Fe. Calcic amphiboles have a variable chemical composition: $(\text{Na}, \text{K})_{0-1} (\text{Na}, \text{Ca}, 2+\text{Mn}, 2+\text{Mg}, 2+\text{Fe})_2 (\text{Mg}, 2+\text{Fe}, 3+\text{Fe}, 2+\text{Mn}, \text{Ti}, \text{Al})_5 (\text{Si}, \text{Al}, 3+\text{Fe})_8 \text{O}_{22} (\text{OH}, \text{O}, \text{F})_2$. In calculating the amphibole composition, the formula is based on 23 oxygen and chlorine combined; and corrected out for hydroxyl anion. Manganese and zinc are less than calculated because of a default minimum in the program on the basis of the standards used. When the results are plotted on compositional diagrams for calcic amphiboles from Ernst, (1968), after Colville et al. (1966), see figures 8, 9, 10, 11 and 12, an intermediate composition is obtained. These figures indicate that the composition contains components of tschermakite to ferrotschermakite, tremolite to ferrotremolite, magnesiohastingsite to hastingsite, and pargasite to ferropargasite. The 2+Fe/(Mg+2+Fe) ratio ranges from 0.4

hornblende apparent age from location 6025 was also partially reset.

Hornblende Composition

Table 5 in the appendix is a compilation of the microprobe results which are used to find the composition of amphiboles. It is found that the amphiboles are calcium amphiboles and fall under the general heading of amphiboles which includes common hornblende, tschermakite, edenite, and pargasite. Since the microprobe determines total iron, the sample formulas have all been calculated on the assumption of 80% 2+Fe and 20% 3+Fe. Calcic amphiboles have a variable chemical composition: $(\text{Na}, \text{K})_{0-1} (\text{Na}, \text{Ca}, 2+\text{Mn}, 2+\text{Mg}, 2+\text{Fe})_2 (\text{Mg}, 2+\text{Fe}, 3+\text{Fe}, 2+\text{Mn}, \text{Ti}, \text{Al})_5 (\text{Si}, \text{Al}, 3+\text{Fe})_8 \text{O}_{22} (\text{OH}, \text{O}, \text{F})_2$. In calculating the amphibole composition, the formula is based on 23 oxygen and chlorine combined; and corrected out for hydroxyl anion. Manganese and zinc are less than calculated because of a default minimum in the program on the basis of the standards used. When the results are plotted on compositional diagrams for calcic amphiboles from Ernst, (1968), after Colville et al. (1966), see figures 8, 9, 10, 11 and 12, an intermediate composition is obtained. These figures indicate that the composition contains components of tschermakite to ferrotschermakite, tremolite to ferrotremolite, magnesiohastingsite to hastingsite, and pargasite to ferropargasite. The 2+Fe/(Mg+2+Fe) ratio ranges from 0.4

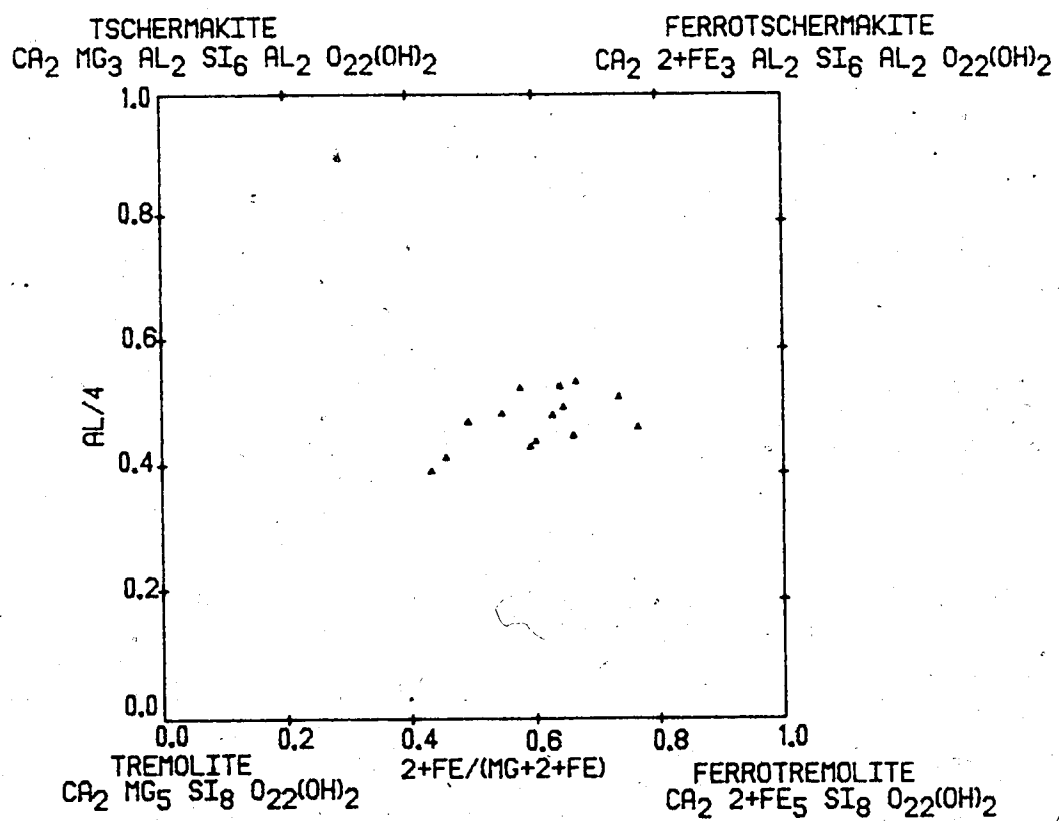


Fig. 8. Distribution of 14 Hill Island Lake amphiboles in the composition range: tremolite-ferrotremolite-tschermakite-ferrotschermakite.

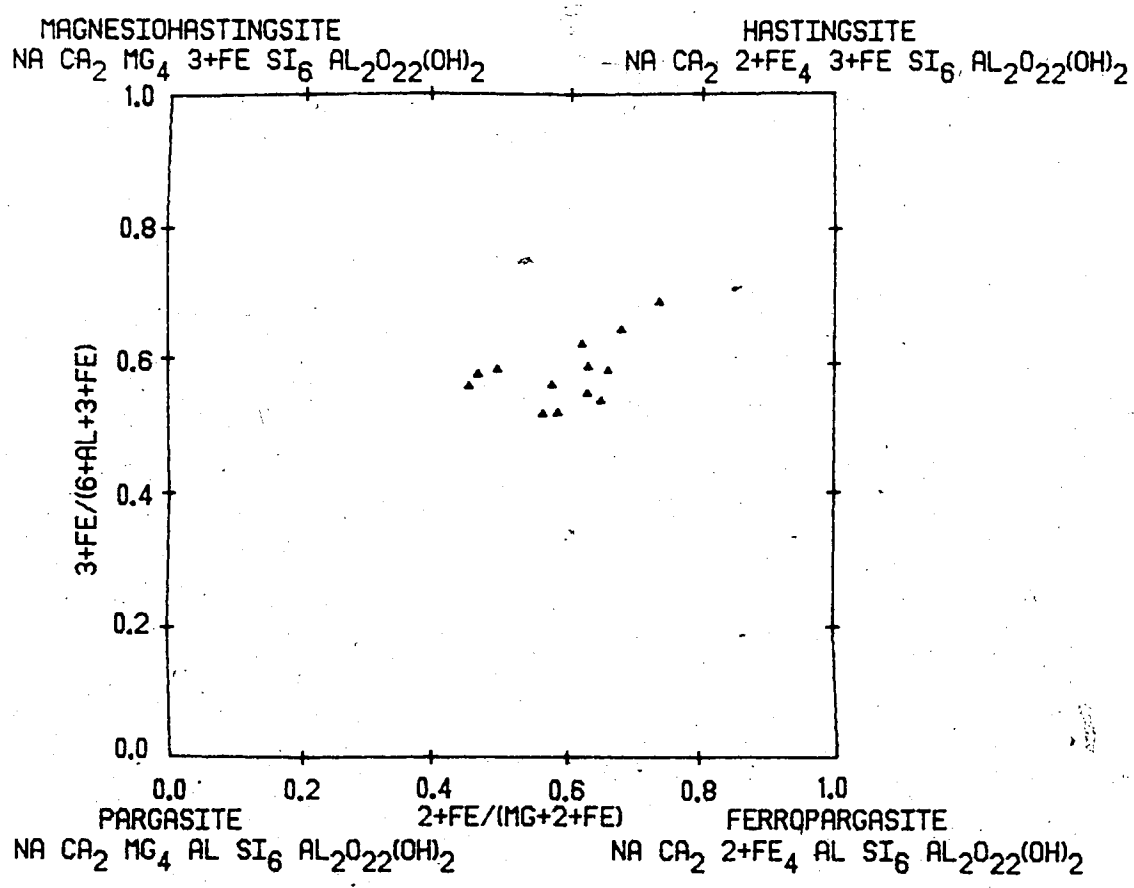


Fig. 9. Distribution of 14 Hill Island Lake amphiboles in the composition range: pargasite-ferropargasite-magnesiohastingsite-hastingsite.

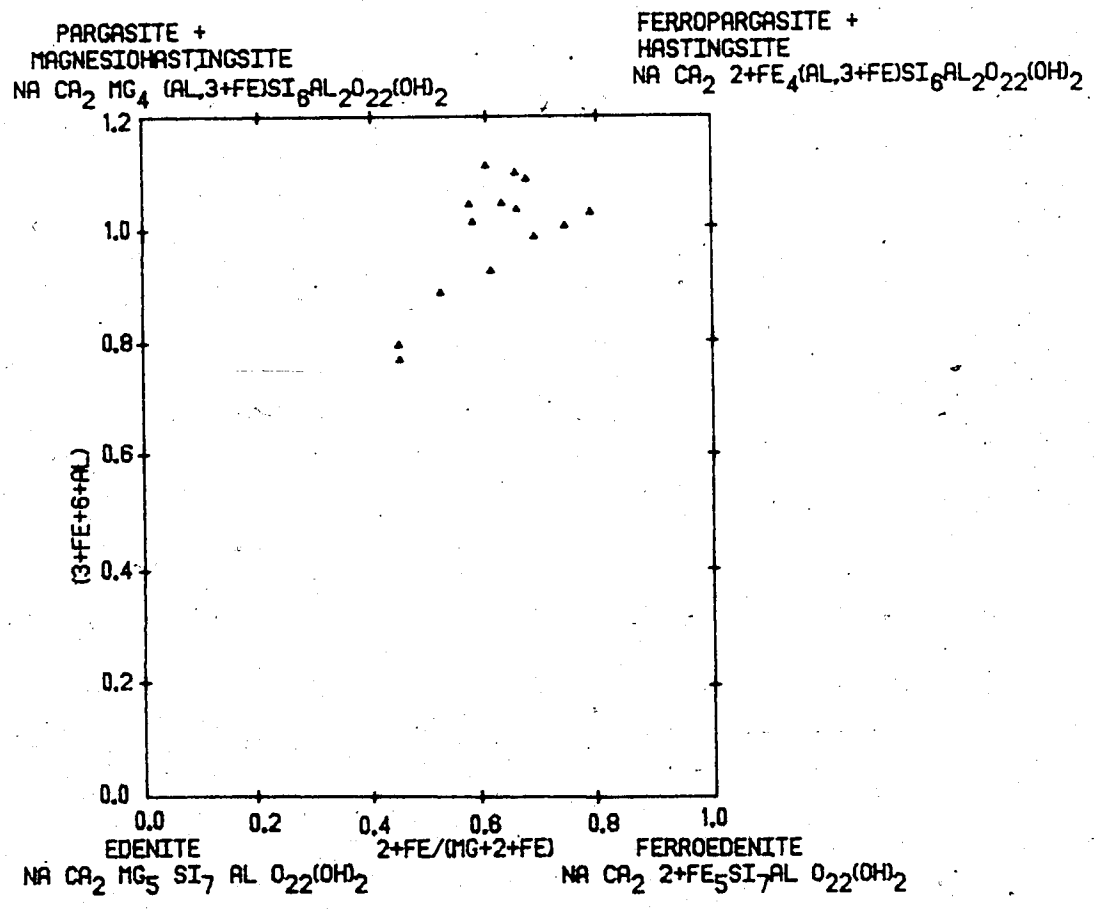


Fig. 10. Distribution of 14 Hill Island Lake amphiboles in the composition range: edenite-ferroedenite- (pargasite+magnesiohastingsite)- (ferropargasite+hastingsite).

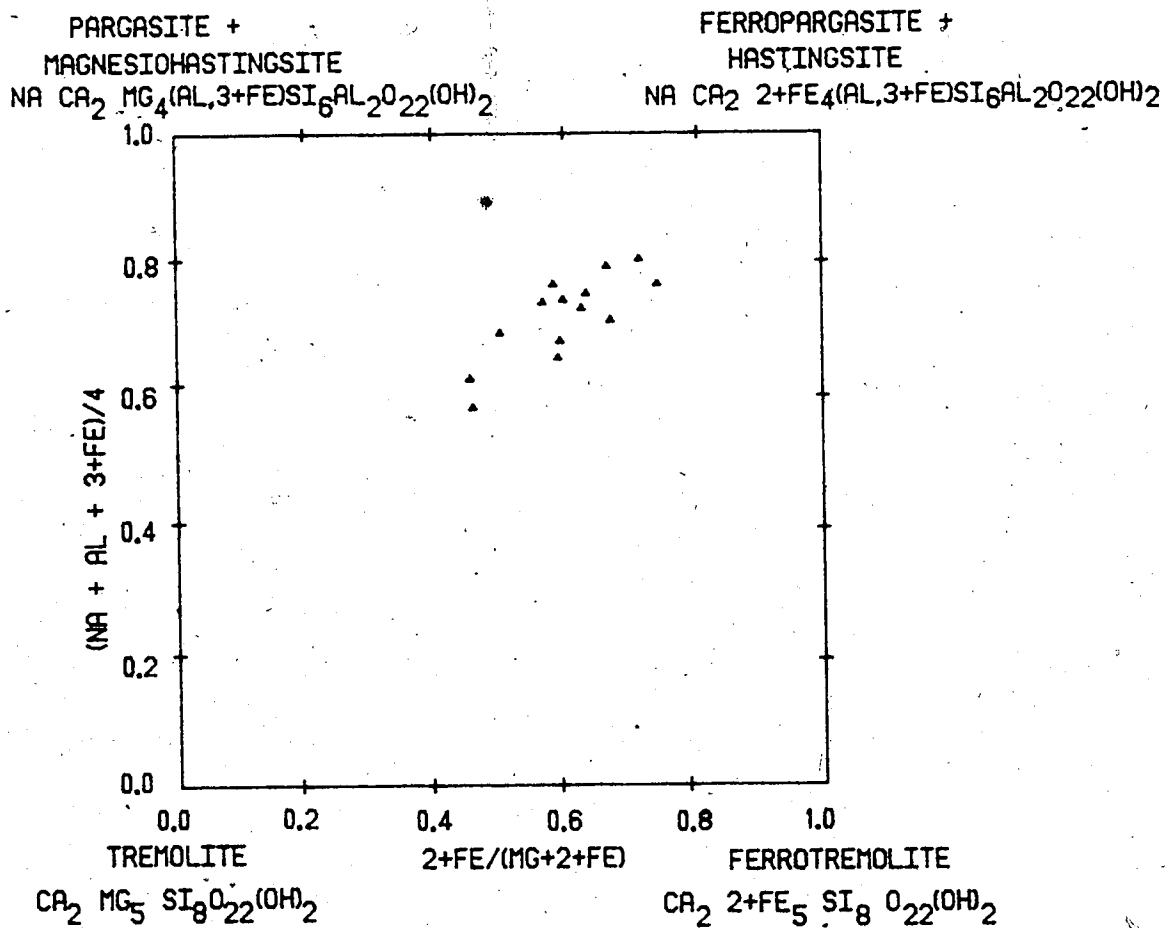


Fig. 11. Distribution of 14 Hill Island Lake amphiboles in the composition range: tremolite-ferrotremolite-(pargasite+magnesiohastingsite)-(ferropargasite+hastingsite).

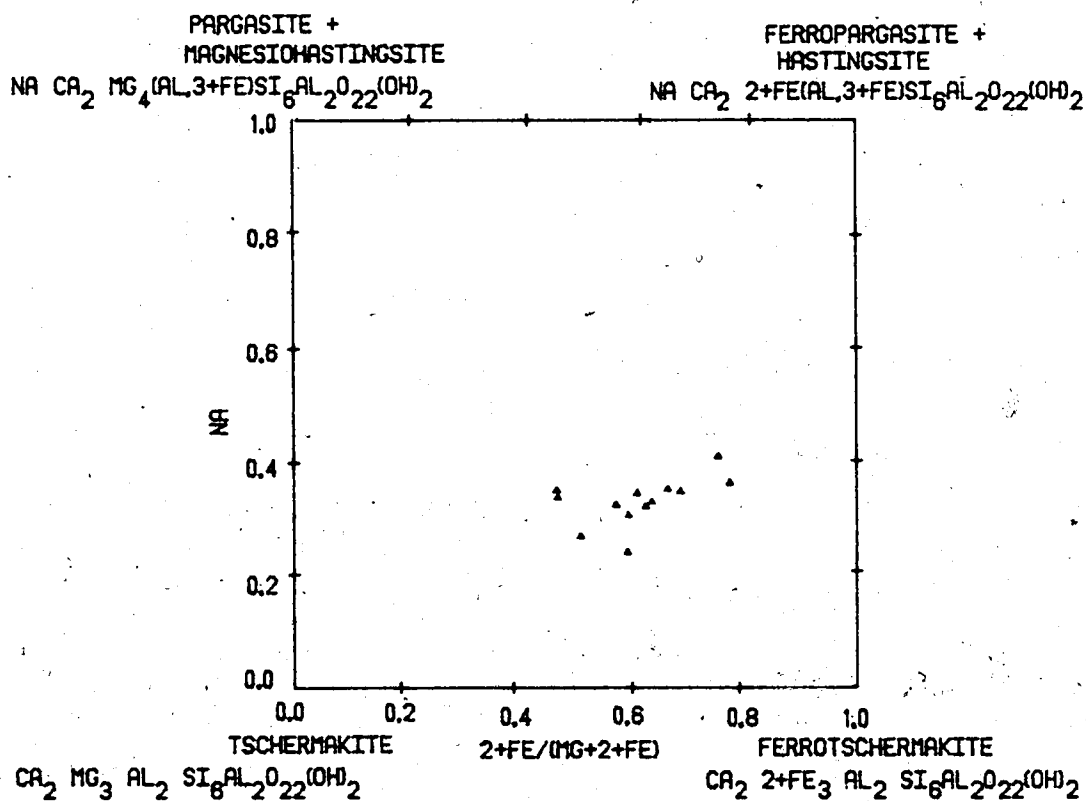


Fig. 12. Distribution of 14 Hill Island Lake amphiboles in the composition range: tschermakite-ferrotschermakite-(pargasite+magnesiohastingsite)-(ferropargasite+hastingsite).

to 0.8, indicating a trend toward iron-rich endmembers and a relatively acidic composition. These trends are consistent with the optical observations and the recognition of tschermakitic amphibole.

The optical observations for amphiboles also indicate a tschermakitic hornblende. For amphiboles, 2V determinations indicate a negative bisectrix with an optic axial angle between 30° and 70°. From Shelley (1975), this range of 2V and O.A.P. orientation for amphiboles appears to fit the hastingsite to Fe-hastingsite compositional field as well as Fe-hornblende, including tschermakite and edenite.

Titanium content in amphiboles has been used as an indicator of metamorphic grade. According to a study by Raase, (1974) high Ti contents suggest higher metamorphic grades. Comparing titanium contents in table 5 with Raase's amphiboles it appears that these amphiboles represent amphibolite to granulite facies metamorphic grade, with an average titanium content of 0.173, although Ti content does not appear to vary with age.

However, the Ti content may not be high relative to the Fe/Ti ratio. When the Fe/Ti ratio is higher, the amphibole color trends toward green to dark green, as is the case with some of the amphiboles in this study. However, when the Fe/Ti ratio is low, the color is brown.

The very low octahedral aluminum content results

from low total alumina in the whole rock and may also represent low pressure genesis.

If high iron represents lower metamorphic grade, then the magnesium end member in the compositional range, which represents higher temperatures of genesis, should also represent higher metamorphic grade.

figure 13, the $2+Fe/(2+Fe+Mg)$ ratio versus apparent age

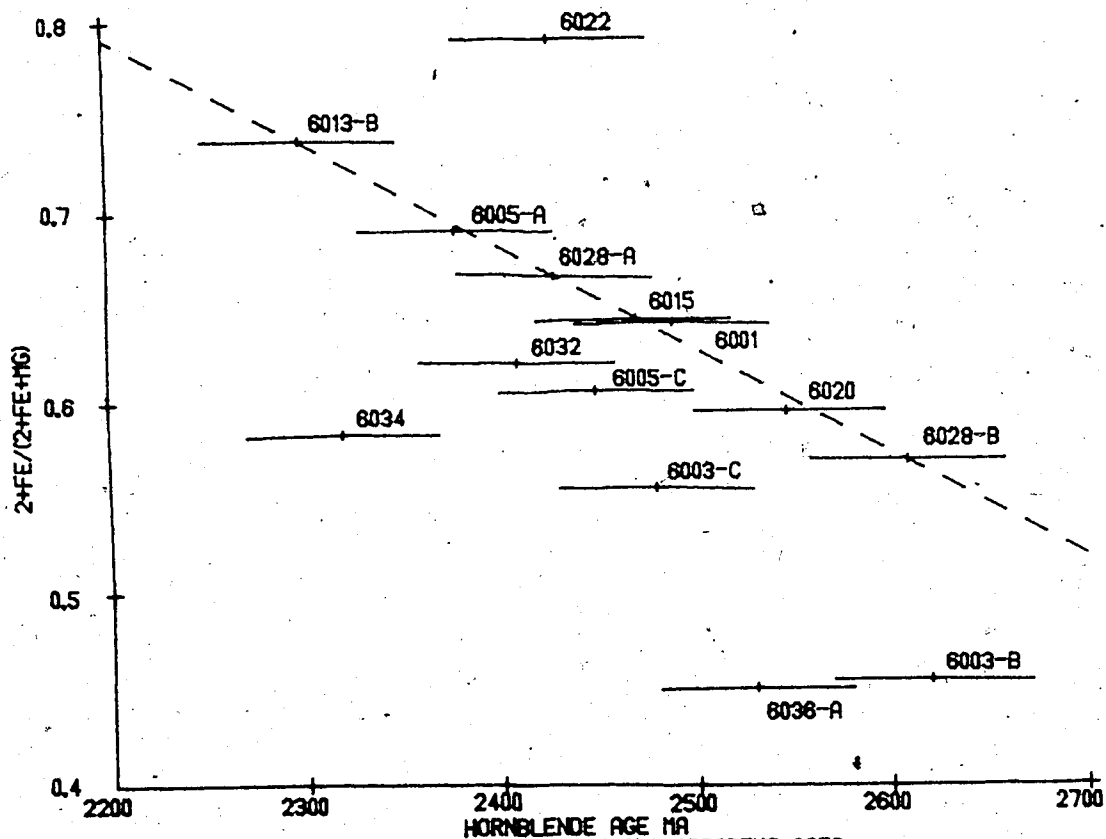


FIG. 13. $2+Fe/(2+Fe+Mg)$ VS. AMPHIBOLE APPARENT AGES.

in amphiboles appears to give an inverse variation with age. The age appears to be unaffected by the iron content below about 0.6, but shows a rough inverse

correlation above 0.6 suggesting a lower retentivity of argon in more iron-rich amphiboles. Evans and Lambert (1974), and O'Nions, Smith, Baadsgaard, and Morton (1969) suggest a similar correlation from Scotland and Norway. Figure 14,

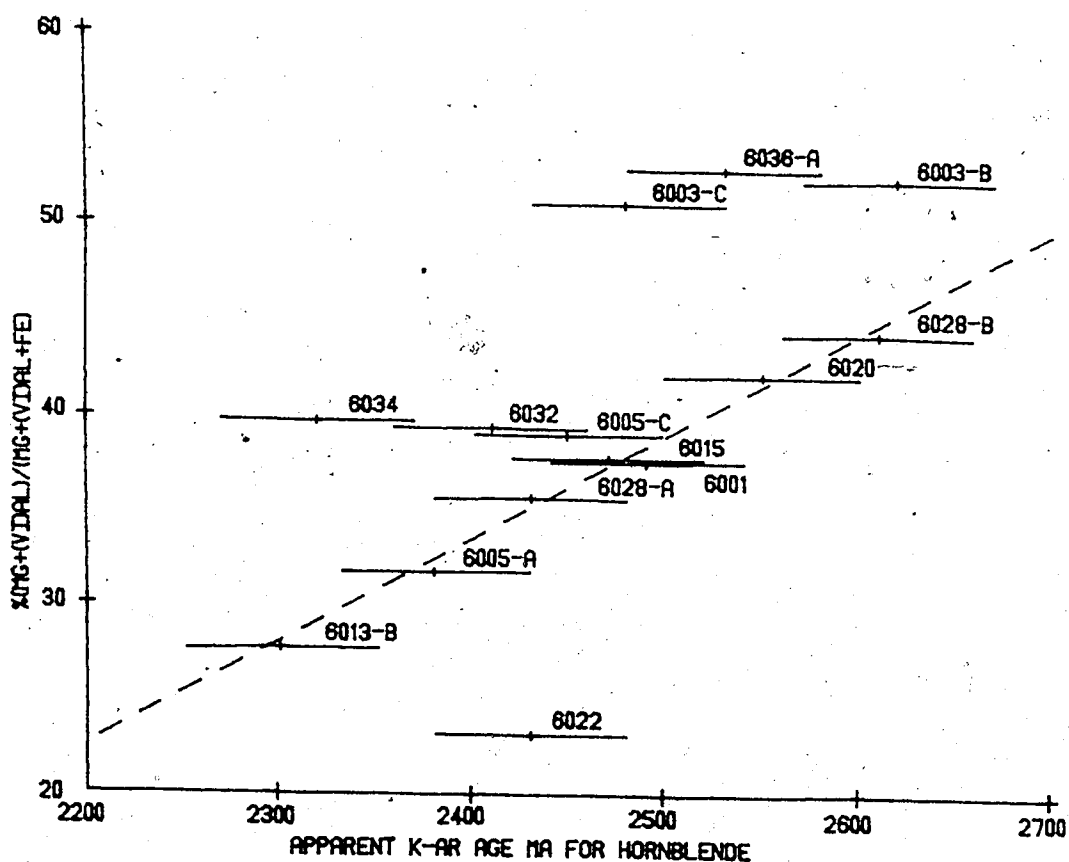


FIG. 14. $\%Mg+(VI)Al/(Mg+(VI)Al+Fe)$ VS. APPARENT K-AR AGE FOR HORNBLLENDE.

the apparent ages for 14 amphiboles versus $\%Mg+Al(VI)/(Mg+Al(VI)+Fe)$ is similar to figure 13 but includes Al(VI) and 3+Fe. The lack of correlation in figure 13 below 0.55 and above 45 in figure 14 may represent a tailing off at or near the maximum

hornblende age, or an early pre-2400 ma resetting. The K-Ar ages of the points lying off the line have been reset by later deformation or later thermal events or both.

The results of figures 13 and 14 are strengthened by the fact that samples from the same location (eg. 6003, 6005 and 6028) give widely different apparent ages, but can be related to compositional difference. These plots suggest that either the amphiboles closed slowly and variably to argon loss as the rocks were slowly uplifted or that a strong later metamorphism partially reset the amphibole ages according to composition. Other factors besides composition not shown in figures 13 and 14, which may have had an effect on hornblende ages are water content including lithology, shearing deformation, and local variations in heating. These rocks appear to have escaped most of the post-2000 ma events because of the dry, competent nature of the rocks already at a high crustal level, and perhaps representing a thicker crustal section than the neighbouring rocks.

C. Conclusions and Discussion

The 2600+ ma basement has been multiply and variably metamorphosed between the time of genesis and 1800 ma, as shown by K-Ar biotite and hornblende apparent ages. The extent of lightly reworked Archean basement is restricted to

the 2200 ma biotite isotherm, which is taken to represent basement not reheated by post-2000 ma events. These post-2000 ma events have remobilized the metasedimentary rocks and the granitic gneisses along the western edge of preserved basement. This remobilization cuts through the northern edge of preserved Archean basement in a northeasterly trending direction. At the northeast corner of the sampled area a second remobilized zone trending northeast cuts into the preserved Archean basement. To the east the boundary is gradational as the rock type becomes predominantly metasedimentary-metavolcanic as deduced from the rock descriptions and geology of neighbouring areas. Also, the band of granulite facies rocks south of Tazin Lake appears to continue into the southeast corner of the Hill Island Lake map area from geologic and structural considerations. The limits of preserved Archean basement are incompletely defined in the northeast corner due to limits of sampling, but the results and magnetic expression, and foliation direction suggest a further extension to the northeast.

Figure 15 is a representation of an approximate sequence of events in the Hill Island Lake and Tazin Lake areas based on K-Ar apparent ages correlated with closing temperature and time. Table 4 is a similar outline of a tectonometamorphic sequence of events for the inlier. After a $2600 \pm$ ma series of intrusive events and granulite facies metamorphism about the time of maximum hornblende apparent

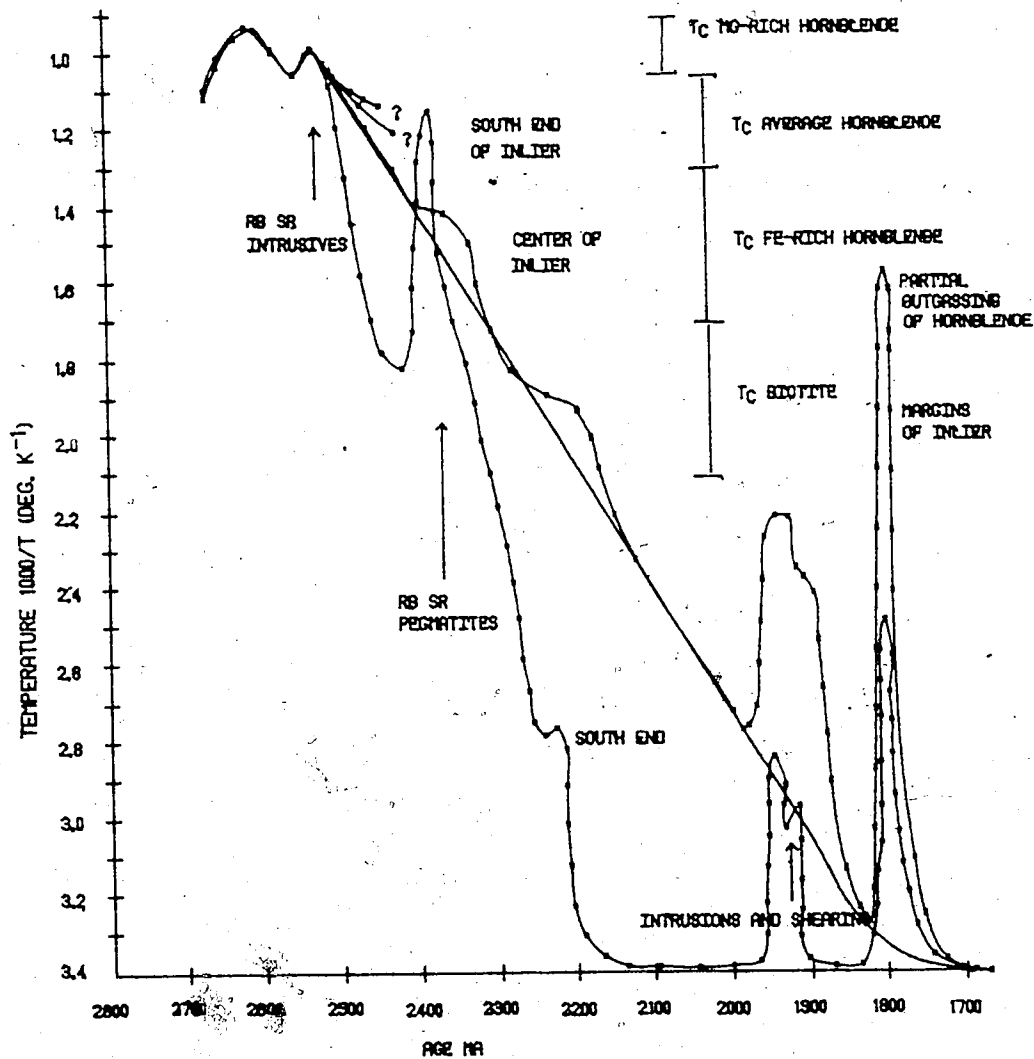


FIG. 15. APPROXIMATE SEQUENCE OF EVENTS

ages, warping and uplift, the area was reheated to upper amphibolite facies, lower granulite facies temperatures during the intrusion of granites, aplogranites and pegmatites at 2533 ± 15 ma. Assuming a maximum $30^\circ\text{C}/\text{km}$ geothermal gradient for established crustal rocks, the rocks in question cooled to amphibolite facies temperatures (550°C) at a maximum depth of about 16 to 20 kilometers

Table 4. A tectonometamorphic sequence of events for the inlier in the Hill Island Lake-Tazin Lake Areas		
Time (ma)	Events	Metamorphism
K-Ar Biot 1950 to 1700	Outside the inlier intrusion of granites, shearing, compression	regional greenschist to granulite, and dynamic
Within the inlier		
K-Ar Biot 2300 to 2200	local heating, uplift	greenschist
K-Ar 2360±40 Rb-Sr 2338±25	local heating associated with late pegmatite intrusion, strong uplift in south part of inlier slow uplift elsewhere	amphibolite cooling rapidly
K-Ar Hbl 2460±95	steady uplift and cooling	amphibolite retrogression
Rb-Sr 2533±15	intrusion of granite, aplogranite, aplite and pegmatite; climactic uplift	lower granulite to upper amphibolite
Rb-Sr 2620±90 K-Ar Hbl 2620±50	intrusion of granodiorite, uplift	granulite local?

sometime during the peak period of hornblende ages about 2400 ma to 2450 ma. The present surface rocks were gradually uplifted and eroded to a maximum depth of about 7 to 10 kilometers by the peak period of biotite ages about 2200 ma. The plateau like contour area shown in maps 1 and 2 of 2200+ ma biotite ages suggests the possibility of a 2250 ma regional thermal event which reset most biotite K-Ar ages in

this area. In addition, biotites north of Tazin Lake were not reset at 2200 ma. This suggests more rapid uplift of the southern end of the inlier before 2250 ma so that these rocks were at a higher crustal level and escaped resetting.

Between Tazin Lake and Portman Lake, rapid uplift, and heating associated with late pegmatite intrusion reset both biotite and hornblende. The uplift possibly in the form of an extended dome as seen on gravity, aeromagnetic, structural, and geology maps raised this area to a much higher crustal level at 2360 ± 40 ma (K-Ar biotite and hornblende), so that the rocks cooled and closed rapidly. There must have been rapid erosion at this time and the formation of immature boulder conglomerates in the surrounding areas such as is seen in the Thekulthili Lake area and south of Stony Rapids. The Rb-Sr ages of Donaldson Lake supracrustals at about 2250 ma (Sassano et al., 1972) and paragneisses in the Charlebois Lake area a maximum Pb/Pb age of about 2300 ma (personal communication Dragon Krstic), support this proposed uplift and formation of a belt of sedimentary rocks around the uplift. The rapid uplift north of Tazin Lake is most likely responsible for the development of the Tazin fault and associated faults. Assuming a constant rate of uplift of about 1 km/25 my., from the closure of hornblende and biotite, these rocks should have neared the surface about 2000 ma. However, there is a peak distribution of biotite ages, at 1950 ma which tails off at 1800 ma. This time of resetting of biotite ages is related

to reworking and remobilization associated with the widespread post-2000 ma events in the Churchill Province. This resetting along the western edge of the area appears to be mainly related to remobilization and argon loss due to shearing. In the north, northeast trending fault systems have reset biotite ages at 1890 to 1960 ma. To the east, a thermal pulse, probably of the same age as the one which produced granulite facies rocks south of Tazin Lake, has partially to completely reset both hornblende and biotite ages. The remainder of the area appears to have escaped post-2000 ma updating due to its competent nature, high crustal level, dry nature, distance from any major thermal activity and relatively thick crust. Major thermal activity appears to have concentrated itself along the Wollaston Lake mobile belt and the Tazin group of metasedimentary rocks which wrap around this granodiorite-diorite basement complex.

The correlation of isotopic with petrographic and structural data appears to be good in so far as the data overlaps with areas in which more detailed work has taken place. The maximum hornblende apparent age correlates well with a Rb-Sr whole rock isochron plot of the country rocks north of Tazin Lake, 2620 ± 90 ma, (Baadsgaard personal communication). The plots of hornblende composition versus apparent age not only indicate a relatively slow rate of cooling and uplift for the basement, but also point to post-2600 ma events that have reset hornblende in this area.

The reset hornblendes correlate with possible resetting events as indicated by petrographic studies and structure. The 2360 ± 40 ma apparent K-Ar ages of biotite and hornblende north of Tazin Lake correlate well with geologic and structural data and 2338 ± 25 ma Rb-Sr pegmatite isochron. Strong uplift in this area associated with granite, aplite and pegmatite intrusion at a Rb-Sr whole rock isochron age of 2533 ± 15 ma, allowed closure to argon loss in biotite to take place much earlier than other areas. Light regional reheating at 2300 to 2200 ma appears to have reset biotite K-Ar apparent ages in the main body of the inlier. Post 2200 ma events are represented by biotite apparent ages outside the inlier. Various late deformational events have reset biotite and in some cases hornblende. These reset ages can be correlated with petrographic and structural features such as mylonitic texture in association with an aeromagnetic low corresponding to a foliation direction. The inlier acted as a stable block during the 1950 to 1700 ma regional reworking and metamorphism, indicating a possible thick competent dry crust, close to the surface at this time.

Speculations

At sample locations 6000 and 6013, the biotite apparent ages are older than the surrounding sample ages while hornblende at location 6013 gives a younger apparent age of 2290 ma. It may be possible that these locations represent intrusive events associated with late pegmatite intrusions.

north of Tazin Lake although more detailed sampling will have to be done as single samples are statistically insignificant.

Areas of positive magnetic relief of 3500+ gammas, see Map 1, may represent more mafic rocks which have been intruded by granites and granodiorites. The aeromagnetic low situated between locations 6027 and 6034 may represent an intrusion of post-2600 ma granite, or aplongranite similar to the one north of Tazin Lake.

In the Hill Island Lake area, at least one fault associated with the Tazin uplift cut the area. One such fault may cut through sample location 6034 as shown by shearing in thin section where the hornblende age may be reset at 2320 ma.

In figure 14, the composition versus age plot assumes that Fe-Mg compositional variation may account for the total age variation encountered although ages will also be affected by local heating, shearing deformation and water content of the hornblendes. Of the points lying off the line both 6003-C and 6034 have been reset by later deformation. 6036-A has been reset by the intrusion of a granite dyke probably of the same genesis as the granite and aplongranite intrusion north of Tazin Lake. 6003-B may have been partially reset by deformation, as well as sample 6005-C. 6032 and 6005 may have been affected by 1800 ma thermal metamorphism as they are situated near the edge of the inlier. It is also possible that these samples have a higher

2+ iron content as compared to total iron, than the rest of the samples. The sample from location 6022 appears to have been involved in the event that reset potassium argon ages in the Tazin Lake area.

If the amphiboles 6003-B, 6003-C and 6036-A in figure 14 are extrapolated to points on the line corresponding to composition, the corresponding apparent ages are 2730 ma, 2710 ma, and 2740 ma. These ages may correspond to the age of granulite facies metamorphism or age of genesis of the rocks. The line may also represent a simple cooling versus age relationship with uplift and cooling culminating at about 1800 ma. This is probable as the biotite ages in the central portion of the inlier appear not to be reset by an 1800 ma event.

These rocks may have been buried deep under piles of 2600 ma intrusive and extrusive rocks, and underplated with granulite facies rocks. Following this burial, an isostatic uplift would have brought the rocks back up near the surface over a long period of time. To test this area for old crust, other methods of age dating should be employed such as Rb-Sr whole rock, Sm-Nd whole rock, and U-Pb zircon and a much larger number of sample ages obtained. Also, more detailed mapping of the geology and structure is necessary for correlation with the isotopic data. This will help sort out the resetting problems involved in this study.

Bibliography

- Abbey, S. and J.A. Maxwell. 1960. Determination of potassium in micas, a flame photometric study: Chemistry in Canada. 12, 37-41.
- Alcock, F.J. 1936. Geology of Lake Athabaska Region. Geol. Surv. Can., Memoir 196.
- Baadsgaard, H. and J.D. Godfrey, 1972. Geochronology of the Canadian Shield in Northeastern Alberta II. Charles - Andrew - Colin Lakes Area. C.J.E.S., 9, 863.
- Beck, L.S. 1966. Structural environment and genesis of the uranium deposits in the Athabasca region, Saskatchewan, Canada. Unpublished Ph.D. thesis, University of Leeds, Leeds, England.
- Beck, L.S., 1969. Uranium deposits of the Athabasca region, Saskatchewan: Sask. Dept. Min. Res. Rept. no. 126.
- Beecham, A.M. 1970. The ABC Fault, Beaverlodge, Saskatchewan. Canadian Journal of Earth Sciences 7, 1264.
- Blake, D.A.W. 1955. Oldman River map area, Saskatchewan: Geological Survey of Canada Memoir 279.
- Burwash, R.A., and H. Baadsgaard. 1962. "Yellowknife-Nonacho Age and Structural Relations" in The Tectonics of The Canadian Shield, (J.S. Stevenson ed.) Roy. Soc. Can. Spec. Publ. 4. U. of Toronto Press, Toronto. p.22-29.
- Camsell, C. 1916. An Exploration of the Fazin and Taltson Rivers, Northwest Territories. Geol. Surv. Can., Memoir 84.
- Christie, A.M., 1952. Goldfields-Martin Lake map area,

- Saskatchewan. Geol. Surv. Canada Mem. 269.
- Cluley, H.J. 1955. The determination of potassium by precipitation as potassium tetraphenylboron and its application to silicate analysis: *The Analyst*, 80, 354-364.
- Coleman, L.C. 1970. Rb/Sr Isochrons for some Precambrian rocks in the Hanson Lake area, Saskatchewan. *C.J.E.S.* 7, 338.
- Colville, P., W.G. Ernst, and M.C. Gilbert, 1966. Relationships between cell parameters and chemical compositions of monoclinic amphiboles: *American Mineralogist*, 51, 1727-1754.
- Cumming, G.L. and B.P. Scott, 1976. Rb-Sr dating of rocks from the Wollaston Lake Belt, Saskatchewan. *C.J.E.S.* 13, 355.
- Cumming, G.L., F. Tsong, and P. Gudjurgis. 1970. Fractional removal of lead from rocks by volatilization. *Earth Planet. Sci. Lett.* 9, 49.
- Damon, P.E. 1968. Potassium argon dating of igneous and metamorphic rocks with applications to the Basin ranges of Arizona and Sonora. In. *Radiometric dating for geologists*. Eds. E.I. Hamilton and R.M. Farquhar. Interscience, London.
- Dalrymple, G.B., and M.A. Lanphere. 1969. *Potassium-Argon Dating: Principles, Techniques, and Applications to Geochronology*. W.H. Freeman and Company, San Francisco. 54-65.

- Dewey, J.F. and R.J. Pankhurst. 1970. The evolution of the Scottish Caledonides in relation to their isotopic age pattern. Transactions of the Royal Society of Edinburgh. Edinburgh
- de Zoysa, T.H. 1974. The Geology of the Ena Lake Area (West Half), Saskatchewan. Sask. Dept. Min. Res. Rept. 142.
- Dodson, H. 1973. Closure Temperature in Cooling Geochronological and Petrological Systems. Contr. Mineral. and Petrol. Springer Verlag. 40, 259-274.
- Ernst, W.G. Amphiboles. Springer-Verlag. New York, 1968.
- Evans, C.R. and R.St.J. Lambert. 1974. The Lewisian of Lochinver, Sutherland; the type area for the Inverian metamorphism. J. of the Geol. Soc., 120, 125-150
- Faure, G. 1977. Principles of Isotope Geology. J. Wiley and Sons, Inc., Toronto. p.151.
- Fraser, J.A. 1978. Metamorphism in the Churchill Province, District of Mackenzie; in Metamorphism in the Canadian Shield, Geol. Surv. Can., Paper 78-10, p. 195-202.
- Gerling, E.K., T.V. Koltsova, B.V. Petrov, and Z.K. Zulfikarova. 1965. On the suitability of Amphiboles for Age determination by the K-Ar method. Geochem. Int., 2, 1, 148.
- Henderson, J.F. 1939. Nonacho Lake, District of Mackenzie. Geol. Surv. Can., Map 526A.
- Hoadley, J.W. 1955. Abitau River, District of Mackenzie. Geol. Surv. Can., Paper 55-10.
- Hutchinson, C.S., 1974. Laboratory Handbook of Petrographic

- Techniques. John Wiley and Sons. New York.
- Koeppel, V., 1968. Age and history of the uranium mineralization of the Beaverlodge area, Saskatchewan: GSC Paper 67-31, 111.
- Koster, F. 1961a. the Thainka Lake area (east half) in Summary of geological surveys conducted in the Precambrian area of Saskatchewan. Cheesman, R.L. et al. ed. p. 25-27.
- Koster, F. 1961b. The geology of the Thainka Lake area (west half) Saskatchewan: Saskatchewan Dept. Mineral Resources Rept. no. 61, 28p.
- Koster, F. 1962a. The geology of the Thainka Lake area (east half) Saskatchewan: Sask. Dept. Mineral Resources Rept. no. 71, 26p.
- Koster, F. 1962b. Harper Lake area (north half) in Summary report of geological surveys conducted in the Precambrian area of Saskatchewan 1962. Cheesman, R.L. ed.: Sask. Dept. Mineral Resources p. 24-25.
- Koster, F. 1963. The Ena Lake area (east half) in Summary report of geological surveys conducted in the Precambrian area of Saskatchewan 1963. Cheesman, R.L. ed.: Sask. Dept. Mineral Resources, p. 23-25.
- Koster, F. 1965a. The geology of the Ena Lake area (east half), Saskatchewan: Sask. Dept. Mineral Resources Rept. no. 91, 31p.
- Koster, F. 1965b. The geology of the Dardier Lake area (west half), Saskatchewan: Sask. Dept. Mineral Resources Rept.

- no. 101, 45p.
- Koster, F. 1968 The geology of the Zin Bay area,
Saskatchewan: Sask. Dept. Mineral Resources Rept. no. 121,
40p.
- Koster, F. 1969. Burchnall Lake area (east half) in Summary
report of geological surveys conducted in the Precambrian
area of Saskatchewan. Cheesman, R.L. ed.: Sask. Dept.
Mineral Resources, p. 9-11.
- Koster, F. 1970. The geology of the Burchnall Lake area,
Saskatchewan: Sask. Dept. Mineral Resources Rept. no.
131, 24p.
- Koster, F. and H. Baadsgaard, 1970. On the geology and
geochronology of northwestern Saskatchewan I. Tazin Lake
region. C.J.E.S. 7, 919.
- Lewry, J.F., and T.I.I. Sibbald. 1977. Variations in
lithology and tectonometamorphic relationships in the
Precambrian basement of northern Saskatchewan. C.J.E.S.
14, 1455.
- Money, P.L. 1965. The geology of the area around Needle
Falls, Churchill River, comprising the Eulas Lake area
(West Half), Sandfly Lake (East Half), and Black Bear
Island Lake area (West Half), Saskatchewan, Sask. Dept.
Min. Resources, Rept. 88.
- Money, P.L., 1966. The geology of the Daly Lake area (East
Half), Saskatchewan. Sask. Dept. Min. Resources, Rept.
108.
- Money, P.L., 1967. The Precambrian geology of the Needle

Falls area, Saskatchewan. Unpublished Ph.D. thesis,
University of Alberta, Edmonton, Alberta.

Money, P.L., A.J. Baer, B.P. Scott, R.H. Wallis. 1970. The
Wollaston Lake belt, Saskatchewan, Manitoba, Northwest
Territories. In: Symposium on basins and geosynclines
the Canadian Shield. A.J. Baer ed. Geol. Surv. Can. Pap.
70-40, 170.

Mulligan, R. and F.C. Taylor. 1969. Hill Island Lake, District
of Mackenzie. Geol. Surv. Can., Map 1203A.

Munday, R.J.C., 1974. The geology of the Dutton Lake area
(East half) Saskatchewan; Sask.DMR Rept. 155.

O Nions, R.K. 1969. Geochronology of Bamble, South Norway.
Unpublished Ph.D. thesis, University of Alberta,
Edmonton, Alberta.

O Nions, R.K., R.D. Morton, and H. Baadsgaard. 1969.
Potassium-argon ages from the Bamble sector of the
Fennoscandian Shield in South Norway. Norsk Geologisk
Tidsskrift, Oslo, 49, 171-190.

O Nions, R.K., G.D.W. Smith, H. Baadsgaard, and R.D. Morton.
1969. Influence of chemical composition on argon
retentivity in metamorphic calcic amphiboles from South
Norway. Earth Planet. Sci. Letters. 15, 339-345.

Peterman, Z.E., 1962. Precambrian basement of Saskatchewan
and Manitoba. Unpublished Ph.D. thesis, Univ. Alberta,
Edmonton, Alberta.

Raase, P. 1974. Al and Ti contents of hornblende, indicators
of pressure and temperature of regional metamorphism.

- Contrib. Mineral. and Petrol. 45, 231-236.
- Sassano, G.P., H. Baadsgaard, and R.D. Morton. 1972. Rb-Sr Isotopic Systematics of the Foot Bay Gneiss, Donaldson Lake Gneiss, and Pegmatite Dikes from the Fay Mine, NW Saskatchewan. C.J.E.S. 9, 11, 1368.
- Shelley, D. Manual of Optical Mineralogy. American Elsevier Publishing Company, Inc: New York, New York, 1975.
- Schrocke, H. 1976. Tschermaksches Molekul-Tschermakite. Neues Jahr. Mineral. Mh. 8, 388.
- Sibbald, T.I.I., R.J.C. Munday and J.F. Lewry. 1976. The Geological Setting of Uranium Mineralization in Northern Saskatchewan: Proceedings of a Symposium held on 10 November 1976. C.E. Dunn (ed.) Saskatchewan Geological Society, Special Publication No. 3.
- Smith, D.G.W. and C.M. Gold. 1979. Edata2: A Fortran IV Computer Program For Processing Wavelength-And/Or Energy Dispersive Electron Microbeam Analyses. D. Newbury (ed). San Francisco Press, San Francisco.
- Stockwell, C.H., J.C. McGlynn, R.F. Emslie, B.V. Sanford, A.W. Norris, J.A. Donaldson, W.F. Fahrig, and K.L. Currie, 1970. Geology of the Canadian Shield in Geol. and Econ. Min. Can. R.J.W. Douglas (Ed.), Econ. Geol. Rep. No. 1, Geol. Surv. Can., pp. 44-150
- Taylor, F.C. 1959. Penylan-Firedrake Lake, District of Mackenzie. Geol. Surv. Can., Map 8-1959.
- Tyrell, J.B. 1896. Report on the Country between Athabasca Lake and Churchill River. Geol. Surv. Can. Ann. Rept.,

New Series, 8, pt. D.

Wanless, R.K. 1969. Isotopic Age Map of Canada, GSC Map
1256A.

Wanless, R.K. and K.E. Eade. 1975. Geochronology of Archean and
Proterozoic rocks in the southern district of Keewatin.
C.J.E.S., 12, 95.

Wanless, R.K., R.D. Stevens, G.R. Lachance and R.N. Delabio.
1970. Age determination and geological studies, K-Ar
isotopic ages. Rept. 9, Geol. Surv. Can. Paper 69-2A.

Wilson, J.T. 1941. Fort Smith, District of Mackenzie. Geol.
Surv. Can., Map 607A.

Wright, G.M. 1957. Geological Notes on Eastern District of
Mackenzie Northwest Territories. Geol. Surv. Can., Paper
56-10.

Appendix

Sample Preparation

The samples collected were crushed, ground, sieved and separated according to the methods described in Hutchinson, (1974). A portion of the sample was saved for hand specimen description and a portion for thin section preparation. The 30 to 100 mesh portion of the sieved sample was used to obtain biotite, muscovite and hornblende mineral separates.

Potassium determinations

Potassium determinations were carried out on biotite and muscovite using the gravimetric method described in Cluley, (1955). Potassium determinations were carried out on hornblende, whole rock, and a few biotite samples using the flame photometer with the volumetric method as described by Abbey and Maxwell (1960). For purposes of correction for biotite contamination, potassium was also determined for grain mounted amphiboles from spectral analysis of energy dispersive microbeam emissions. This technique and the program for calculation of chemical composition is described by Smith and Gold (1979).

Argon determinations

Argon determinations were accomplished by extraction with mineral decomposition, isotope dilution and purification in a glass argon train as described in Dalrymple and Lanphere, (1969).

Spikes, Reagents and Constants

The spikes used for argon determinations were approximately 2×10^{-5} cc. STP 38 argon. The reagents used for potassium gravimetric method are 1:10 dilute sodium tetraphenyl boron ($\text{Na}[\text{B}(\text{C}_6\text{H}_5)_4]$) solution prepared by mixing NaOH and AlCl_3 and purified using $\text{Al}(\text{OH})_3$. The other reagents used to dissolve and extract potassium from the mineral separates are 5 mls. of HF and 2 mls. of 1N H_2SO_4 .

For volumetric determination of potassium the aliquot was compared to a standard NBS, 1975 containing 192.33ug/g of 41K, and 3.7ug/g of 39K with atomic proportions of: 39K = 0.929371, 41K = 0.07051, 40K = 0.0001193.

Constants used for calculation are: $40\text{K}/\text{K}(\text{total}) = 1.167 \times 10^{-4}$, $\lambda_\epsilon = 0.581 \times 10^{-10}$, $\lambda_\beta = 4.962 \times 10^{-10}$, ppm 40K = $(\% \text{K} 20 \times 93.36) \div 94.2$, age (ma) = $(10,000 \div 5.543) \times \ln[((40\text{Ar}/40\text{K} \times 5.543) \div 0.581) + 1]$. Air argon atomic fractions used are: $40\text{Ar} = 0.996$, $38\text{Ar} = 0.00063$, $36\text{Ar} = 0.00337$ and atomic ratios are: $40/36 = 295.5$, $40/38 = 1581$, $38/36 = 0.1869$. The spike ratios for argon are $40/38 = 0.0021219$, $36/38 = 0.0000727$.

Microprobe Analysis

The microprobe analysis was performed on grain mounted hornblende samples and chemical compositions have been calculated as mentioned in the section on potassium determinations. The results of this analysis are presented in Table 5.

Table 5 Composition of Amphiboles

Sample No.		
6001		
Element	Oxide Wt%	Structural formula based on 23(O,C1)
H	3.819	0.0
O		23.0000
Na	1.068	0.3240
Mg	5.827	1.3595
Al	11.130	2.0533
Si	41.071	6.4289
Cl	0.0	0.0
K	1.376	0.2748
Ca	10.379	1.7407
Ti	1.052	0.1239
Mn	0.392	0.0520
2+Fe	18.627	2.4384
3+Fe	5.173	69.154
Zn	0.082	0.0095

Sample No.

6003-B

Element	Oxide Wt%	Structural formula
H	3.812	0.0
O		22.9790
Na	1.127	0.3326
Mg	9.521	2.1604
Al	9.128	1.6377
Si	43.837	6.6733
K	1.150	0.2233
Ca	10.580	1.7257
Ti	1.968	0.2253
Mn	0.528	0.0680
2+Fe	14.246	1.8136
3+Fe	3.958	0.4534
Zn	0.084	0.0094
Cl	0.081	0.0210

Sample No.

6003-C

Element	Oxide Wt%	Structural formula
H	4.734	0.0
O		22.9667
Na	0.949	0.2847
Mg	9.683	0.2847
Al	30.657	1.9439
Si	41.482	6.4200
Cl	0.127	0.0333
K	1.032	0.2037
Ca	9.265	1.5364
Ti	1.550	1.804
2+Fe	15.431	1.9972
3+Fe	4.287	0.4993
Zn	0.190	0.0217

Sample No.

6005-A

Element	Oxide Wt%	Structural formula
H	3.505	0.0
O		23.0000
Na	1.151	0.3508
Mg	5.045	1.1820
Al	9.728	1.8023
Si	41.581	6.5362
Cl	0.0	0.0
K	1.349	0.2705
Ca	10.170	1.7129
Ti	1.1464	0.1730
Mn	0.339	0.0451
2+Fe	19.966	2.6247
3+Fe	5.547	0.6562
Zn	0.154	0.0179

Sample No.

6005-C

Element	Oxide Wt%	Structural formula
H	3.585	0.0
O		23.0000
Na	1.139	0.3430
Mg	6.533	1.5119
Al	9.525	1.7429
Si	42.514	6.6008
Cl	0.0	0.0
K	1.233	0.2442
Ca	10.576	1.7593
Ti	1.559	0.1820
Mn	0.445	0.0585
2+Fe	17.850	2.3178
3+Fe	4.959	0.5794
Zn	0.081	0.0093

Sample No.

6013-B

Element	Oxide Wt%	Structural formula
H	4.042	0.0
O		23.0000
Na	1.325	0.4100
Mg	4.033	0.9595
Al	10.910	2.0525
Si	39.363	6.2835
Cl	0.0	0.0
K	1.688	0.3438
Ca	10.010	1.7119
Ti	2.059	0.2471
Mn	0.458	0.0620
2+Fe	20.378	2.7204
3+Fe	5.662	0.6801
Zn	0.073	0.0086

Sample No.

6015

Element	Oxide Wt%	Structural formula
H	4.124	0.0
O		23.0000
Na	1.092	0.3326
Mg	5.553	1.2996
Al	11.615	2.1496
Si	40.273	6.3240
Cl	0.0	0.0
K	1.621	0.3247
Ca	10.460	1.7598
Ti	1.865	0.2203
Mn	0.503	0.0668
2+Fe	17.807	2.3385
3+Fe	4.948	0.5846
Zn	0.139	0.0161

Sample No.

6020

Element	Oxide Wt%	Structural formula
H	3.968	0.0
O		23.0000
Na	0.805	0.2410
Mg	6.915	1.5919
Al	9.798	1.7836
Si	43.694	6.7489
Cl	0.0	0.0
K	0.683	0.1347
Ca	9.562	1.5825
Ti	0.609	0.0707
Mn	0.587	0.0768
2+Fe	18.180	2.3948
3+Fe	5.051	0.5987
Zn	0.147	0.0168

Sample No.

6022

Element	Oxide Wt%	Structural formula
H	4.093	0.0
O		23.0000
Na	1.186	0.3686
Mg	3.234	0.7729
Al	9.805	1.8532
Si	40.289	6.4607
Cl	0.0	0.0
K	1.411	0.2886
Ca	10.090	1.7336
Ti	1.624	0.1958
Mn	0.489	0.0665
2+Fe	21.630	2.9007
3+Fe	6.010	0.7252
Zn	0.140	0.0166

Sample No.

6028-A

Element	Oxide Wt%	Structural formula
H	3.911	0.0
O		22.9738
Na	1.131	0.3462
Mg	5.265	1.2387
Al	11.928	2.2189
Si	39.660	6.2596
Cl	0.098	0.0262
K	1.718	0.3460
Ca	10.422	1.7624
Ti	1.275	0.1514
Mn	0.429	0.0574
2+Fe	18.824	2.4847
3+Fe	5.230	0.6212
Zn	0.129	0.0150

Sample No.

6028-B

Element	Oxide Wt%	Structural formula
H	4.939	0.0
O		23.0000
Na	1.051	0.3185
Mg	7.033	1.6382
Al	10.923	2.0120
Si	41.535	6.4912
Cl	0.0	0.0
K	1.264	0.2520
Ca	10.458	1.7511
Ti	1.301	0.1529
Mn	0.269	0.0356
2+Fe	16.540	2.1618
3+Fe	4.595	0.5404
Zn	0.091	0.0105

Sample No.

6032

Element	Oxide Wt%	Structural formula
H	4.956	0.0
O		23.0000
Na	1.049	0.3210
Mg	6.061	1.4262
Al	10.632	1.9782
Si	41.086	6.4862
Cl	0.0	0.0
K	1.395	0.2810
Ca	10.463	1.7698
Ti	1.129	0.1340
Mn	0.482	0.0645
2+Fe	17.766	2.3455
3+Fe	4.936	0.5864
Zn	0.044	0.0051

Sample No.

6034

Element	Oxide Wt%	Structural formula
H	4.077	0.0
O		22.9870
Na	1.151	0.3502
Mg	6.220	1.4553
Al	14.553	2.1374
Si	40.118	6.2972
C	0.049	0.0130
X	1.747	0.3498
Ca	10.514	1.7682
Ti	1.615	0.1907
Mn	0.365	0.0485
2+Fe	17.581	2.3079
3+Fe	4.885	0.5770
Zn	0.137	0.0159

Sample No.

6036-A

Element	Oxide Wt%	Structural formula
H	4.601	0.0
O		23.0000
Na	1.199	0.3552
Mg	9.676	2.2031
Al	8.702	1.5666
Si	44.361	6.7764
Cl	0.0	0.0
K	0.863	0.1682
Ca	10.415	1.7046
Ti	1.701	0.1954
Mn	0.221	0.0286
2+Fe	14.220	1.8166
3+Fe	3.951	0.4541
Zn	0.090	0.0102

Error Analysis

A number of errors are involved in determinations. These include measuring the respective biotite potassium ($\pm 1\%$), hornblende potassium ($\pm 0.1\%$), biotite argon ($\pm 0.15\%$), and hornblende argon ($\pm 0.15\%$). The accuracy of results was not known because of indeterminate errors. To estimate the overall or total precision, the reproducibility of K-Ar results from Northeast Alberta was calculated. Results from this area measure the apparent age of different minerals which may be used to find a maximum variation in age for both hornblende and biotite. Age determinations for the Albertan samples and this study were run on the same instruments by the same operators during a concurrent time period. For 100 samples run at about the same time as the present study, the standard deviation in the apparent age is ± 20 my. For a 2 sigma variation (± 40 my.), approximately 95% confidence, the reproducibility is $\pm 2\%$ of 1790 ma. For a 2500 ma age in this study the corresponding reproducibility is ± 50 my.

Thin Section Descriptions

From forty nine thin sections the common rock type present can be depicted. The essential constituents are most commonly plagioclase, quartz and potassium feldspar, and occasionally biotite and hornblende. The anorthite content of the plagioclase ranges from 5% to about 40% (albite to andesine), most commonly 20-25% (oligoclase), with one quarter of the rocks less than An17. Plagioclase can

constitute as much as 70% of the rock. Quartz is present as an essential mineral in all rocks except amphibolites where it is varietal. It ranges up to 60% of the rock components. Potassium feldspar is microcline and orthoclase, ranging in content from 0% to 60%. Biotite is seldom an essential mineral but is almost ubiquitous. It ranges in content from 15% to 0%. It mostly occurs as a varietal mineral and as a secondary alteration of hornblende. A number of thin sections show two generations of biotite. Hornblende occurs as an essential mineral in five thin sections usually in amphibolites but occurs mainly as a varietal mineral in eighteen thin sections. As discussed in the interpretations, its composition is tschermakitic and the hornblende is often poikilitic containing biotite, quartz, epidote, magnetite, apatite and K-feldspar.

Other varietal minerals not already mentioned are muscovite, sphene, apatite, magnetite and epidote. Normally these are accessory minerals in most of these rocks but are quite abundant in about one quarter of these rocks. They are often found as inclusions in hornblende and plagioclase or intergrown with them.

Accessory minerals consist of nearly all the above mentioned minerals as well as zircon, garnet, rutile, allanite, tourmaline, pyrite, hematite. Most of these minerals only occur in a few thin sections except zircon.

Secondary minerals consist of chlorite, zoisite, clinozoisite, sericite, carbonate and biotite. These

minerals are alteration products of plagioclase, biotite, hornblende and rarely potassium feldspar.

Special features include the presence of myrmekite, perthite, antiperthite, microgranite, poikilitic hornblende containing biotite and corroded zircons.

The texture of these rocks ranges from polygonal, through crush, breccia, porphyroblastic, granoblastic, protocataclastic, hartshiefer, protomylonitic, blastomylonitic, cataclastic to mylonitic. Where porphyroblasts are preserved from shearing they are mostly common potassium feldspar.

A few of these rocks exhibit relict pyroxene, pseudomorphs of hornblende and biotite after pyroxene. Occasionally a trace of clinopyroxene (diopside) is found.

A general modal analysis of each sample from the Hill Island Lake area is presented here.

(6001) Granodioritic Gneiss

Foliated, augen gneiss with xenoliths, with antiperthite and hornblende altered to clinozoisite, biotite, and carbonate. The plagioclase averages An 23. Biotite is slightly altered to chlorite. Modal analysis is: Pl 40, Qz 30, Kfd 13, Bi 9, Hb <1.

(6002) Quartz Monzonite (Feldspar Porphyry)

Porphyritic, granoblastic, leucocratic rock containing with plagioclase averaging An 30. Biotite is altered to chlorite. Modal analysis is: Pl 50, Qz 25, Kfd 15, Bi 4.

(6003-A) Monzonitic Augen Gneiss

Protomylonitic, fine grained, augen, gneiss containing plagioclase with average An 20. Biotite is slightly altered to chlorite, and plagioclase to sericite, epidote and carbonate. Modal analysis is: Pl 60, Qz 10, Kfd 10, and Bi 13.

(6003-B) Pegmatite

Pegmatite layer from same location as 6003-A containing microcline antiperthite and with a crush texture. Microcline is altered to chlorite and sericite. Modal analysis is: Pl 72, Qz 10, Kfd 8, Hb 2.

(6003-C) Pegmatite

Pegmatite from same location as 6003-B but with more alteration. Hornblende is altered to epidote and biotite. The plagioclase averages An 17, lower than the other pegmatite, and contains a vein of muscovite cutting through the quartz and feldspar. Modal analysis is: Pl 72, Qz 10, Kfd 5, Hb 4, Ep 3.

(6004) Granitic Gneiss

Protomylonitic, augen gneiss containing antiperthite and myrmekite and K-feldspar augens. Modal analysis is: Qz 35, Kfd 35, Pl(An 15) 15, Bi 10.

(6005-A) Granitic Gneiss

Mesocratic, cataclastic, granitic gneiss much altered with plagioclase average An 24. Hornblende contains biotite inclusions both along and across cleavage. Modal analysis is: Kfd 52, Qz 15, Pl 13, Bi 10, Hb 5, Cpx? <1, Ap 2.

(6005-B) Pegmatitic Granitic Gneiss

Cataclastic, pegmatitic gneiss containing graphic granite and relict pyroxene. Biotite altered slightly to chlorite, plagioclase appears to be albite. Modal analysis is: Mi 62, Qz 20, Pl 10, Bi 3, An 1

(6005-C) Granodioritic Gneiss

Poikilitic, protocataclastic, sphene rich, hornblende, biotite gneiss containing relict pyroxene and plagioclase An 24-35. Hornblende contains epidote, biotite, and magnetite, and a quartz vein cuts through the rock. Modal analysis is: Pl 45, Bi 15, Qz 10, Hb 10, Kfd 5, Sph 2.

(6005-D) Granodioritic Gneiss

Protocataclastic gneiss with relict hornblende and muscovite vein cutting through. Hornblende is altered to biotite, carbonate, and chlorite. Modal analysis is: Pl(An 20) 45, Bi 15, Qz 10, Kfd 10, Hb 10.

(6006) Quartz Dioritic Gneiss

Schistose gneiss containing perthite, relict amphibole, and sphene and apatite with biotite. Biotite is strongly altered to chlorite and sericite. Modal analysis is: Pl(An 24), Qz 15, Bi 5, Mi 2, Sph 2, Ap 2, Chl 2.

(6007) Granodioritic Gneiss with Pegmatitic Segregations

Crush to breccia textured gneiss with remobilized quartz and feldspar and augens of feldspar. Hornblende is altered to epidote, carbonate and biotite and biotite is slightly altered to chlorite. Modal analysis is: Pl(An 26-38) 55, Qz 20, Kfd 15, Bi 3, Hb 1.

(6008) Monzonitic Gneiss

Cataclastic, melanocratic gneiss containing microcline perthite, myrmekite, and plagioclase (An 18) containing biotite. Biotite is slightly altered to chlorite, and hornblende is slightly altered to carbonate. Modal analysis is: Pl 55, Qz 15, Hb 12, Bi 10, Mi 1, Zr 2, Ap 2.

(6009) Granodioritic Gneiss

Blastic, cataclastic to hartshiefer gneiss with quartz remobilized in veins, contains perthite. Biotite is altered to chlorite and plagioclase is altered to epidote. Modal analysis is: Pl 55, Qz 45, Pl 27, Mi 15, Bi 5, Ch 1.

(6010-A) Granitic Gneiss

Protomylonitic gneiss containing pyrite, microcline antiperthite, perthite, and myrmekite. Hornblende is altered to biotite is altered to chlorite. Modal analysis is: Pl (An 13-17) 45, Qz 22, Mi 20, Bi 3, Hb 2, Py 2.

(6010-A?) Quartz Dioritic Gneiss

Mylonitic to cataclastic gneiss with zoned plagioclase (An 22-28), strongly recrystallized quartz and myrmekite. Plagioclase is moderately altered to sericite, epidote and carbonate, biotite is slightly altered to chlorite, and hornblende contains magnetite, biotite and epidote. Modal analysis is: Pl 50, Qz 30, Bi 4, Mi 2, Hb 1, Ch 1.

(6010-B) Amphibolite Dyke

An east-west striking dyke which cuts the previously described gneisses and is physically undeformed, is altered, hornblende to biotite (3%), and carbonate, and plagioclase (An 28-34) to epidote and sericite. Modal analysis is: Pl

55, Hb 25, Mi 5, Bi 5, Qz 3, Ep 2.

(6011) Mesocratic Gneiss

Gneissose, protocataclastic, syenitic gneiss with relict amphibole and pyroxene, contains abundant apatite and magnetite and is strongly altered. Plagioclase (An 14-19) is strongly altered to sericite and clinozoisite, biotite is strongly altered to pinitite and sericite, and hornblende is altered to carbonate. Hornblende, biotite, chlorite, quartz and plagioclase are intergrown. Modal analysis is: Pl 50, Hb 13, Mi 10, Bi 5, Qz 3, Ap 3, Cpx <1, Clzo 5, Ch 3.

(6012) Granodioritic Gneiss

Schistose, blastomylonitic to protomylonitic, melanocratic gneiss with pegmatitic layers contains biotite and feldspar porphyroclasts, and a symplectic intergrowth of biotite and quartz. Plagioclase is altered to clinozoisite, sericite and carbonate, biotite is slightly altered to sericite. Modal analysis is: Pl (An 20-30) 55, Qz 25, Bi 7, Kfd 5, Hb 2.

(6013-A) Granitic Gneiss with Pegmatite

Polygonal to aligned possibly recrystallized quartz in gneiss, containing symplectic intergrowths of biotite, quartz and orthoclase. Biotite contains inclusions of zircon and apatite. Modal analysis is: Pl (An 16) 35, Or 40, Qz 15, Bi 3, Hb 2.

(6013-B) Pegmatitic Granitic Gneiss

Granoblastic to polygonal gneiss containing myrmekite, biotite quartz symplectites, two biotites and quartz with

seriate grain boundaries. Modal analysis is: Pl (An 18-20) 55, Or 25, Qz 15, Bi 3, Hb <1.

(6014) Granite

Crush to blastomylonitic granite cut by quartz veins and altered, plagioclase (An <8) to carbonate, sericite and epidote, biotite to chlorite. Modal analysis is: Qz 40, Pl 35, Mi 15, Bi 3.

(6015) Granodioritic Gneiss

Blastomylonitic to protocataclastic augen gneiss containing microcline antiperthite and metamict zircons. Biotite is altered to chlorite. Hornblende contains biotite and quartz. Modal analysis is: Qz 30, Pl (An 15-20) 25, Mi 20, Bi 15, Hb 5.

(6016) Quartz Diorite

Blastomylonitic to mylonitic with microcline porphyroblasts, containing antiperthite, zoned zircons and relict hornblende. Biotite is slightly altered to epidote, chlorite and sericite. Modal analysis is: Pl (An 28) 65, Bi 15, Qz 10, Mi 3, Ep 1.

(6017) Granodioritic Gneiss

Porphyroblastic, crush, epidote rich gneiss containing myrmekite. Biotite is altered to chlorite. Modal analysis is: Pl (An 36) 55, Qz 20, Kfd 15, Bi 4, Ep 3.

(6018) Granite

Porphyroblastic, crush, granite containing microcline antiperthite, myrmekite and biotite in plagioclase. Modal analysis is: Pl (An 5-15) 50, Qz 35, Mi 5, Bi 5, Musc 2.

(6019) Granite

Porphyroblastic to crush granite containing antiperthite and perthite. The biotite is strongly altered to chlorite and sericite. Modal analysis is: Pl 35, Or+Mi 30, Qz 15, Bi 2, Ep 1, Ap 2, Hem 1, Chl 7.

(6020) Quartz Dioritic Gneiss

Cataclastic, chloritic gneiss cut by aplite veins, containing plagioclase (An 30) with pericline twinning. hornblende contains biotite and epidote alteration and apatite. Biotite is slightly altered to chlorite. Modal analysis is: Pl 40, Qz 40, Bi 7, Hb 5.

(6021) Granite

Cataclastic to blastomylonitic, leucocratic granite containing microcline with biotite inclusions. Biotite is altered to chlorite. Modal analysis is: Qz 45, Mi 35, Pl (An 10-20) 15, Bi 3.

(6022) Granite

Crush textured granite containing microgranite and a trace of antiperthite. Hornblende contains biotite along cleavages, and also plagioclase, apatite, carbonate, magnetite and epidote. Modal analysis is: Qz 37, Pl (An 22) 25, Kfd 25, Bi 5, Hb 1.

(6023-A) Granite

Crush textured granite containing microcline antiperthite, microgranite, and stringers of biotite, muscovite and microcline. Modal analysis is: Pl (An 10-25) 35, Qz 30, Mi 25, Bi 3, Musc 2.

(6023-B) Granite

Brecciated, pegmatitic, quartz rich granite containing microcline with muscovite inclusions. Modal analysis is: Qz 60, Mi 25, Pl 10, Bi 2, Musc 1.

(6024) Granite

Brecciated, leucocratic granite containing microgranite. Biotite is altered to chlorite and sericite. Modal analysis is: Qz 35, Pl 35, Mi 20, Bi 2.

(6025) Amphibolite Gneiss

Crush textured gneiss containing plagioclase (An 26-46) with inclusions of biotite and quartz, and hornblende with inclusions of epidote, apatite, biotite, and magnetite. Biotite is slightly altered to chlorite. Modal analysis is: Pl 55, Qz 15, Hb 15, Bi 10, Ep 2.

(6026) Granitic Gneiss

Crushed and foliated gneiss containing microcline antiperthite and interstitial muscovite veining. Modal analysis is: Pl 30, Qz 30, Mi 30, Musc 5, Bi 2.

(6027-A) Monzonitic Gneiss

Cataclastic, leucocratic gneiss with some alteration, biotite to chlorite. Modal analysis is: Qz 35, Mi 30, Pl (An 28) 25, Bi 5.

(6027-B) Granitic Gneiss

Blastomylonitic gneiss containing recrystallized quartz. Biotite is slightly altered to chlorite. Modal analysis is: Qz 55, Mi 30, Pl 10, Bi 3.

(6028-A) Granodioritic Gneiss

Crushed gneiss cut by pegmatite dyke containing abundant antiperthite, myrmekite, relict pyroxene and poikilitic hornblende. Hornblende contains biotite and apatite and is altered to epidote. Biotite is slightly altered to chlorite. Modal analysis is: Pl (An 20-24) 65, Qz 10, Mi 8, Bi 7, Hb 5, Ap 2.

(6028-B) Amphibolite Gneiss

Hartshiefer gneiss containing hornblende with biotite inclusions and alterations, and biotite altered to chlorite. Modal analysis is: Pl (An 12-25) 65, Hb 15, Bi 7, Qz 3, Ap 2.

(6029) Quartz Monzonitic Gneiss

Blastomylonitic, augen gneiss containing perthite. Hornblende contains biotite and biotite is altered to chlorite. Modal analysis is: Pl (An 17-37) 30, Kfd 30, Qz 30, Bi 4, Hb 1.

(6030) Quartz Dioritic Gneiss

Protomylonitic gneiss with streaks of pegmatite. Biotite is strongly altered to phlogopite, sericite and chlorite. Modal analysis is: Pl (An 25-35) 50, Qz 35, Bi 5, Kfd 4, Musc 2.

(6031) Granodioritic Gneiss

Well foliated, crush gneiss containing microgranite. Biotite is altered to chlorite and sericite. Modal analysis is: Qz 40, Pl (An 17-34) 35, Mi 20, Bi 4, Chl 5.

(6032) Granodioritic Gneiss

Chloritized, crush, mesocratic gneiss containing

microgranite, perthite and relict hornblende. Biotite is strongly altered to sericite and chlorite. Modal analysis is: Pl (An 18-31) 40, Qz 35, Mi 15, Bi 5, Mte 1, Ser 3, Chl 1.

(6034) Biotite Schist

Blastomylonitic 'schist' containing perthite, antiperthite, recrystallized quartz and poikilitic hornblende with inclusions of quartz, biotite, and feldspar. Biotite is altered to chlorite. Modal analysis is: Pl (An 28-30) 50, Qz 20, Kfd 10, Bi 10, Hb 5, Ep 2, Chl 2.

(6035) Granitic Gneiss

Protomylonitic, mesocratic gneiss containing myrmekite, microgranite, perthite, antiperthite and poikilitic hornblende with inclusions of biotite and apatite. Alteration is hornblende to carbonate and epidote. Modal analysis is: Pl (An 14-17) 55, Qz 20, Kfd 10, Bi 5, Hb 3, Ep 2.

(6036-A) Amphibolite

Massive, polygonal rock containing poikilitic hornblende with inclusions of quartz and apatite and intergrown with magnetite and biotite. Modal analysis is: Hb 50, Pl (An 14) 35, Qz 3, Mte 3, Bi 2.

(6036-B) Granite

Polygonal, leucocratic granite containing quartz with seriate grain boundaries. Modal analysis is: Mi 60, Qz 15, Pl (An 27) 15, Bi 2, Chl 1.

Plate I. Hornblende with contaminant

a. Sample no. 6001. hornblende with biotite and epidote inclusions. transmitted light, green filter, magnification X 16.

b. Sample no. 6005-A. hornblende with biotite inclusions along cleavage and across cleavage. transmitted light, green filter, magnification X 50.

PLATE I.



a



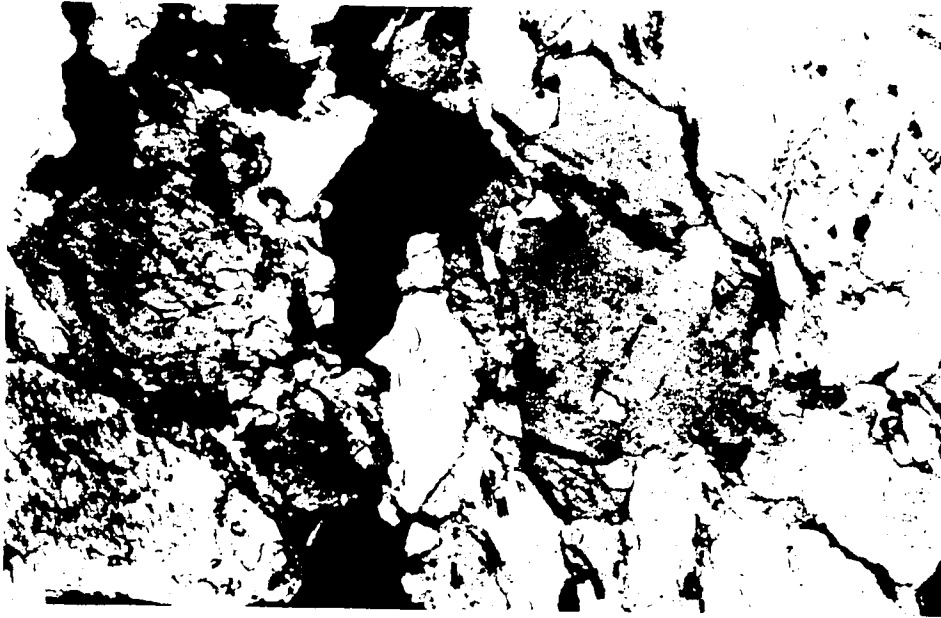
b

Plate II. Hornblende, magnetite, biotite and quartz intergrowth

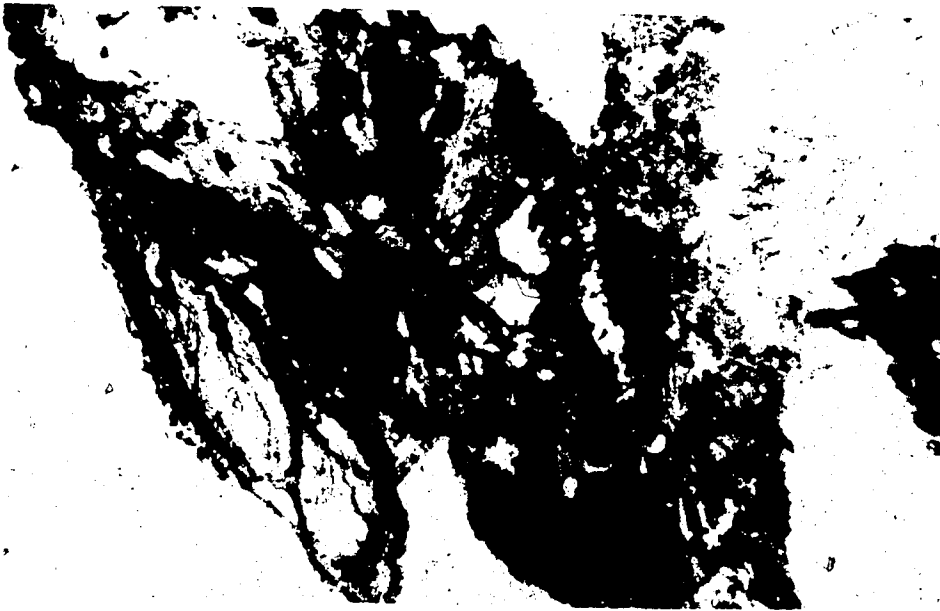
a. Sample no. 6010-A. intimate association of hornblende, magnetite, biotite, and quartz with epidote alteration. transmitted light, yellow filter, magnification X 40.

b. Sample no. 6010-A(?). hornblende, magnetite, biotite, and quartz intergrown with biotite altering to chlorite. transmitted light, yellow filter, magnification X 12.5.

PLATE II.



a



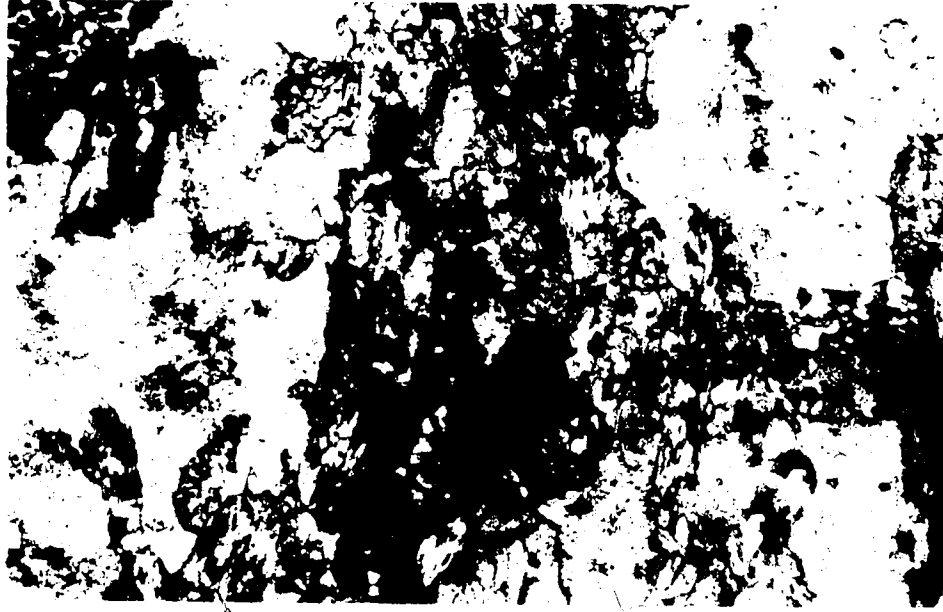
b

Plate III. Hornblende, biotite intergrowth and biotite in plagioclase

a. Sample no. 6011. amphibole, biotite, chlorite, quartz and plagioclase intergrown and altered. transmitted light, green filter, magnification X 16.

b. Sample no. 6018. biotite inclusion in plagioclase. transmitted light, green filter, magnification X 16.

PLATE III.



a



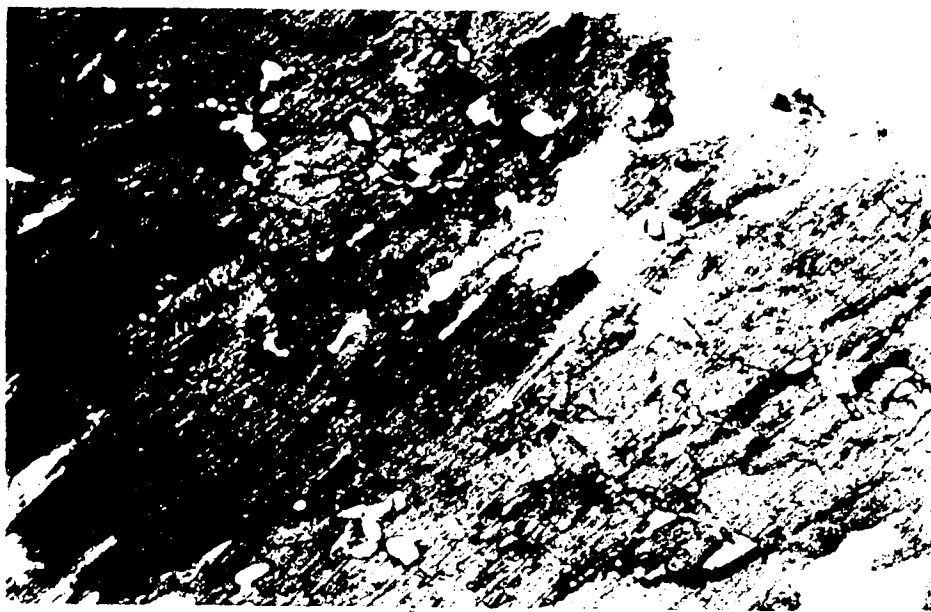
b

Plate IV. Hornblende with intergrowth of minerals

a. Sample no. 6022. hornblende with biotite along cleavages; plagioclase, apatite, carbonate, magnetite and epidote. transmitted light, green filter, magnification X 10.

b. Sample no. 6025. amphibole with inclusions of epidote, apatite, biotite and magnetite. transmitted light, green filter, magnification X 40.

PLATE IV.



a



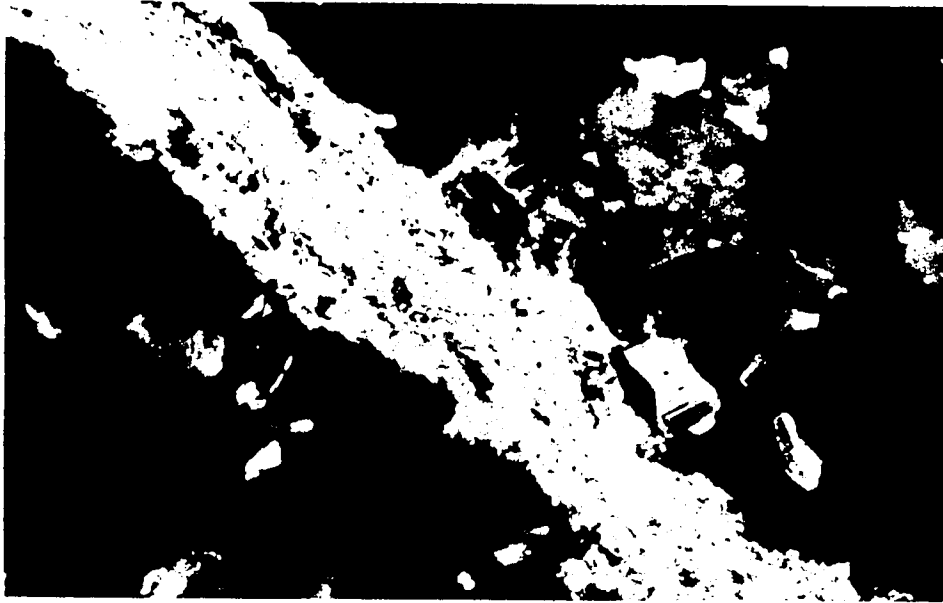
b

Plate V. Polymetamorphism and biotite alteration

a. Sample no. 6026. muscovite vein interstitial with biotite against plagioclase and quartz. Some antiperthite present. transmitted light, crossed polars, yellow filter, magnification X 10.

b. Sample no. 6033. strongly chloritized biotite with associated muscovite, magnetite and plagioclase. transmitted light, crossed polars, yellow filter, magnification X 40.

PLATE V



a



b

Plate VI. Amphibolite facies retrogression and alteration

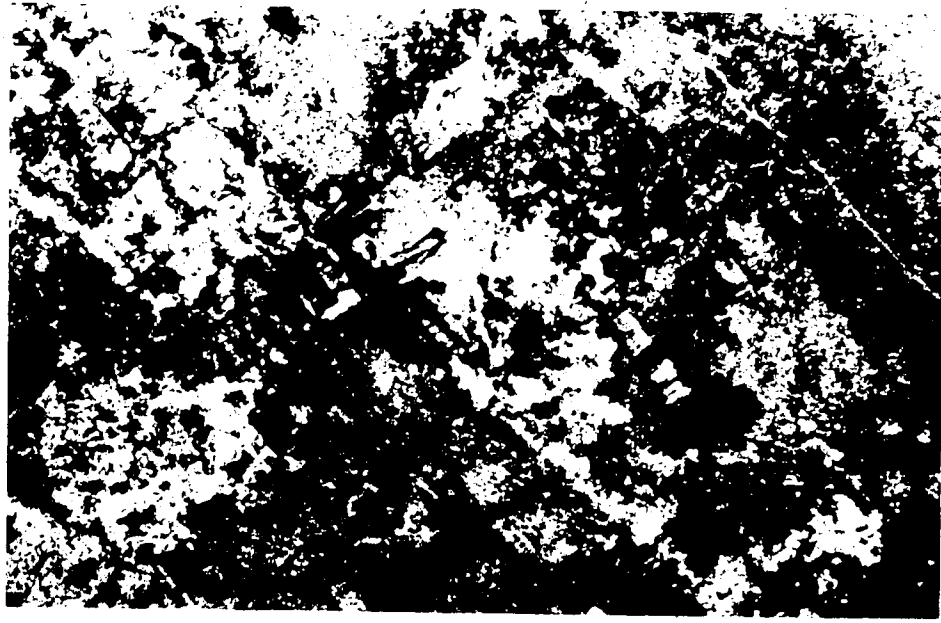
a. Sample no. 6036-A. hornblende intergrown with magnetite and biotite which is altering to sericite. transmitted light, pale green filter, magnification X 10.

b. Sample no. 6001. microcline with altered plagioclase. Plagioclase altered to sericite and epidote. Perthite present. transmitted light, yellow filter, magnification X 10.

PLATE VI.



a



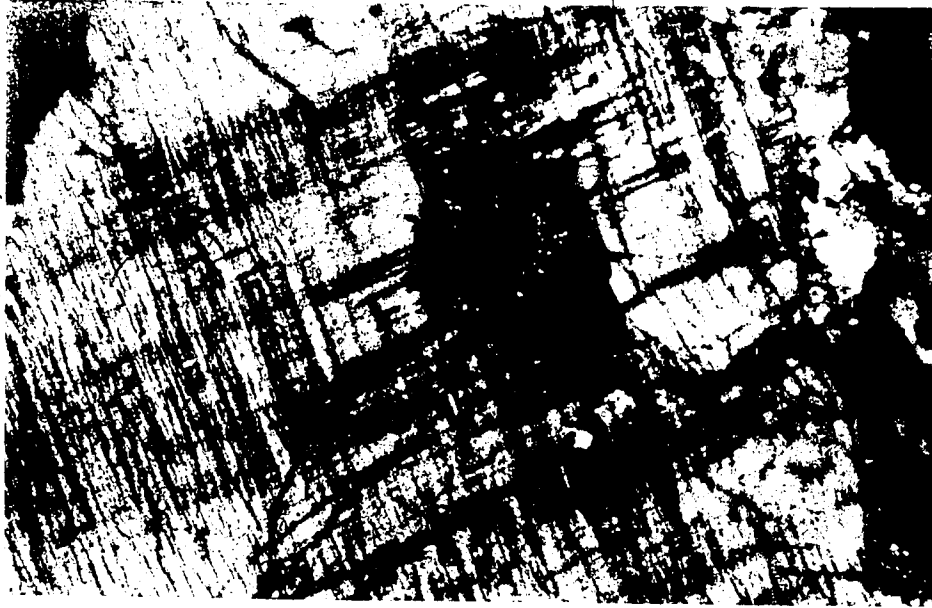
b

Plate VII. Granulite facies retrogression and deformation

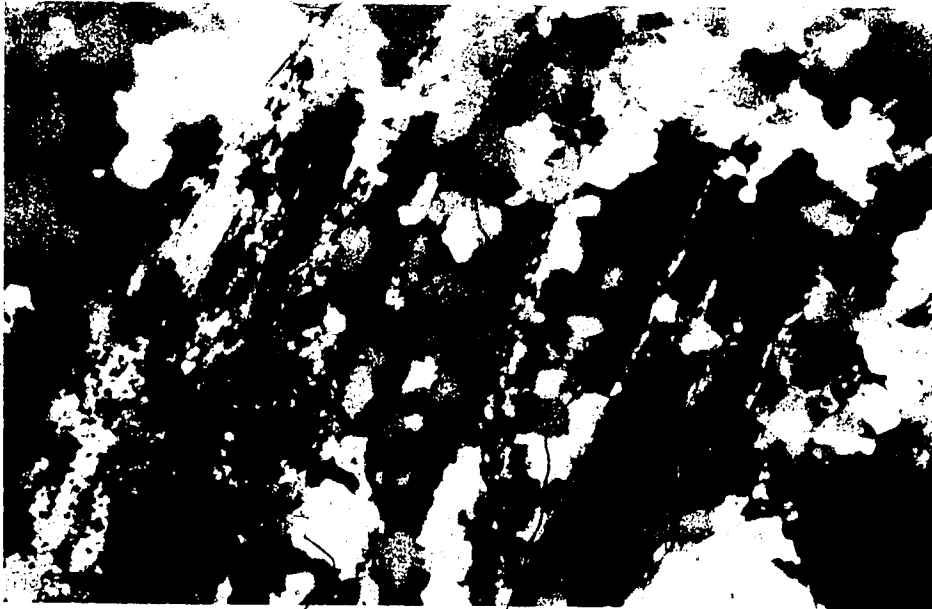
a. Sample no. 6003-C. antiperthite altered to epidote and sericite. transmitted light, yellow filter, magnification X 10.

b. Sample no. 6004. protomylonite texture. Biotite with quartz. transmitted light, yellow filter, magnification X 10.

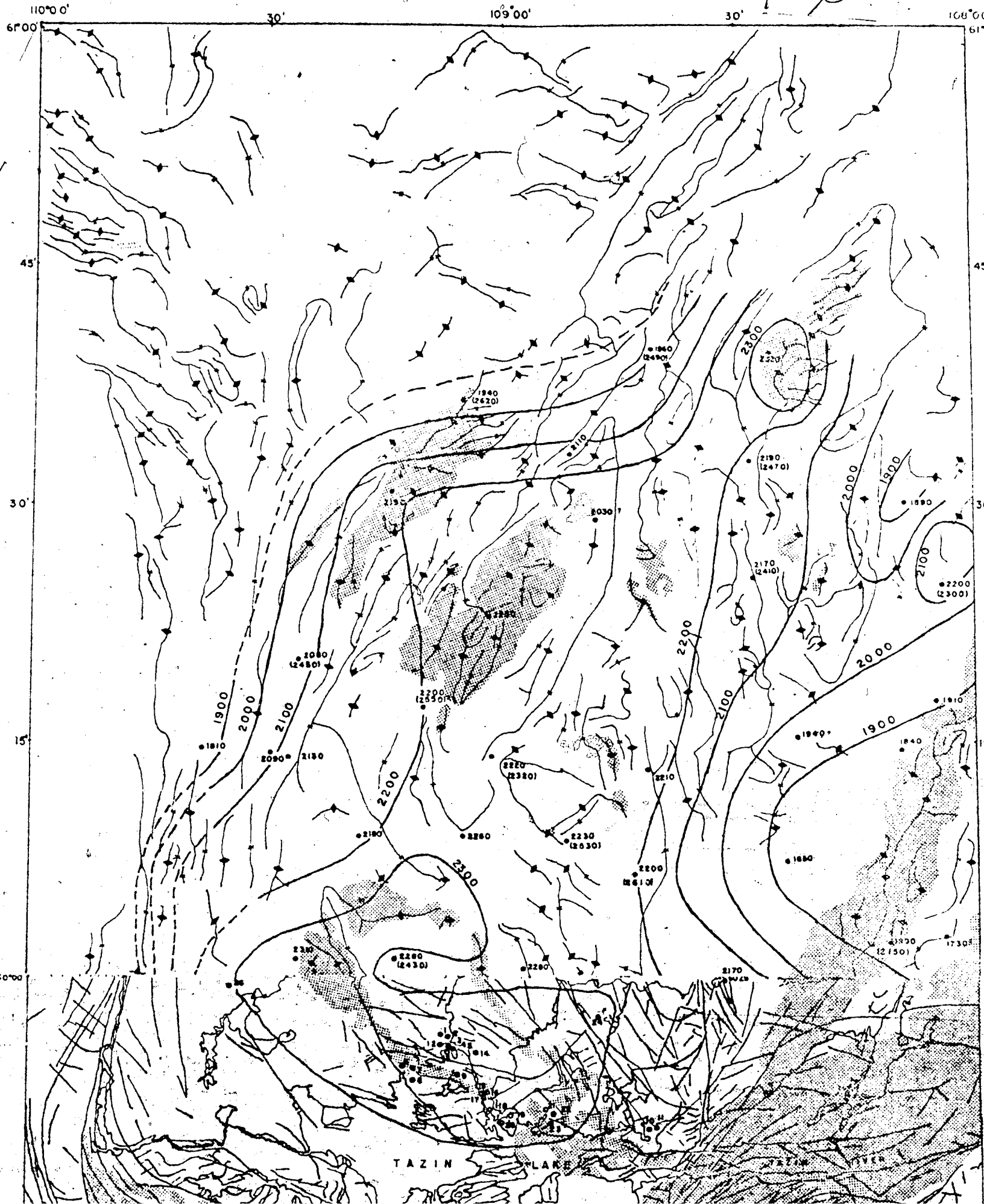
PLATE VII.

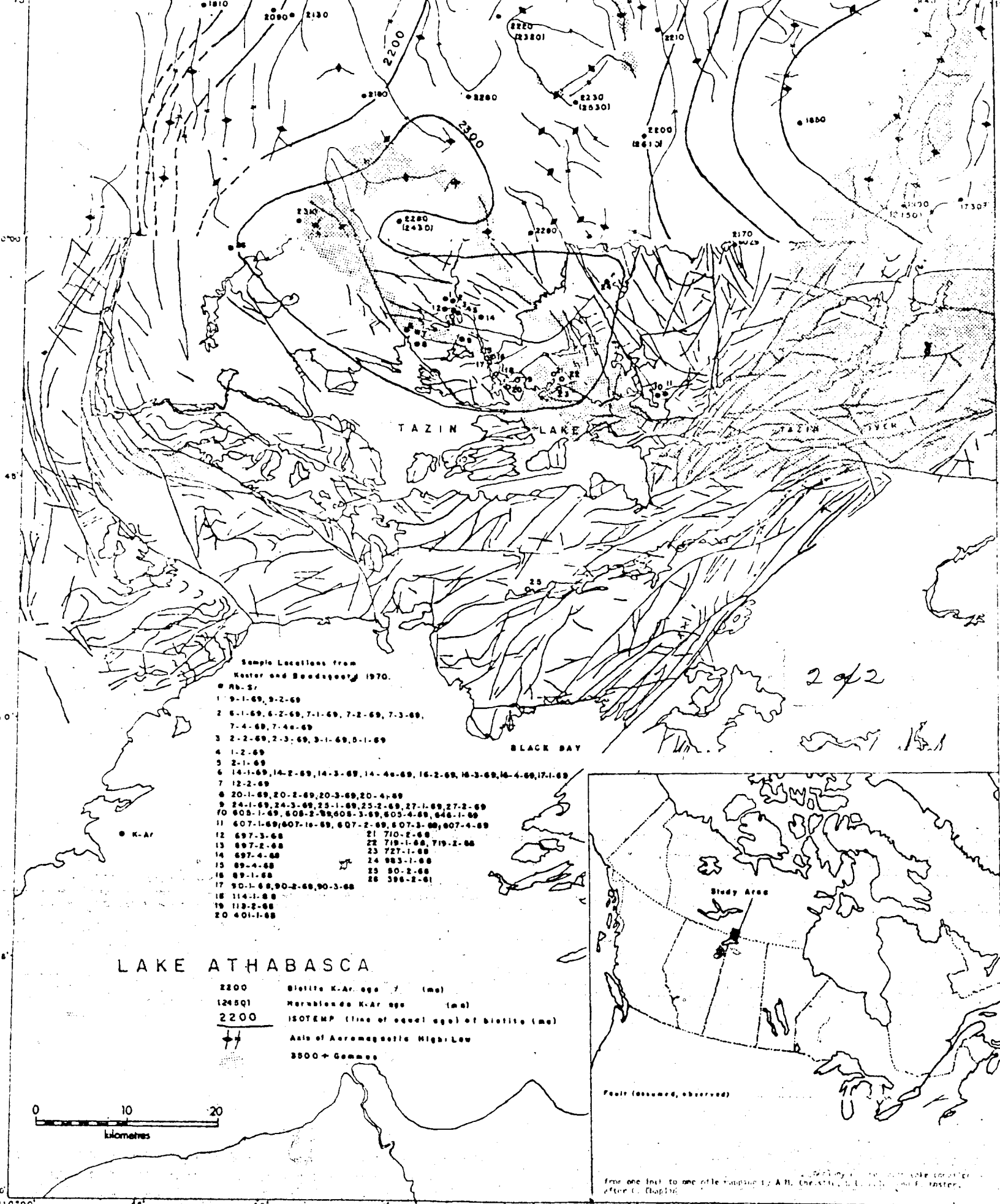


a



b





- Sample Locations from
Kester and Sandegard, 1970.
- Rb-Sr
- 1 9-1-69, 9-2-69
 - 2 6-1-69, 6-2-69, 7-1-69, 7-2-69, 7-3-69,
7-4-69, 7-4a-69
 - 3 2-2-69, 2-3-69, 3-1-69, 5-1-69
 - 4 1-2-69
 - 5 2-1-69
 - 6 14-1-69, 14-2-69, 14-3-69, 14-4a-69, 16-2-69, 16-3-69, 16-4-69, 17-1-69
 - 7 12-2-69
 - 8 20-1-69, 20-2-69, 20-3-69, 20-4-69
 - 9 24-1-69, 24-3-69, 25-1-69, 25-2-69, 27-1-69, 27-2-69
 - 10 603-1-69, 603-2-69, 603-3-69, 605-4-69, 646-1-69
 - 11 607-1-69, 607-1a-69, 607-2-69, 607-3-69, 607-4-69
 - 12 697-3-68 21 710-2-68
 - 13 697-2-68 22 719-1-68, 719-2-68
 - 14 697-4-68 23 727-1-68
 - 15 89-4-68 24 983-1-68
 - 16 89-1-68 25 80-2-68
 - 17 90-1-68, 90-2-68, 90-3-68 26 396-2-61
 - 18 114-8-68
 - 19 113-2-68
 - 20 401-1-68

LAKE ATHABASCA

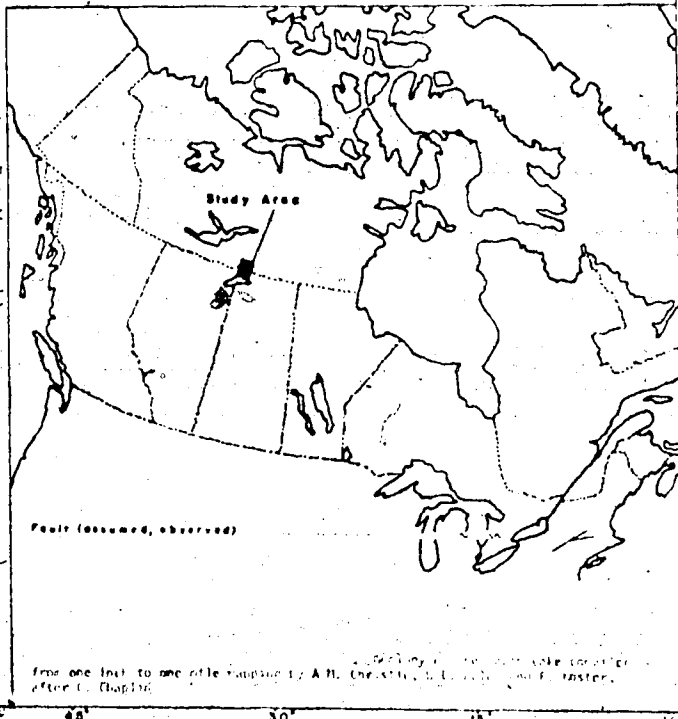
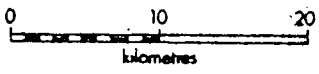
2200 Biotite K-Ar age 7 (ma)

1245Q1 Muscovite K-Ar age (ma)

2200 ISOTEMP (line of equal age) of biotite (ma)

++ Axis of Aeromagnetic High-Low

3500+ Contour



From one inch to one mile map by A.H. Christie, U.L. and G.H. Kester, after C. Chaplin

